

Cooldown capability of Ringhals 3 residual heat removal system

A transient numerical simulation from 4 hours to 36 hours after reactor shutdown

Master's Thesis within the Sustainable Energy Systems programme

JAKOB DOTEVALL

JENNIE NORDKVIST

Department of Energy and Environment
Division of Energy Technology
CHALMERS UNIVERSITY OF TECHNOLOGY
Göteborg, Sweden 2012
Report no. T2012-374

MASTER'S THESIS

Cooldown capability of Ringhals 3 residual heat removal system

A transient numerical simulation from 4 hours to 36 hours after reactor shutdown

Master's Thesis within the Sustainable Energy Systems programme

JAKOB DOTEVALL

JENNIE NORDKVIST

SUPERVISOR:

Tobias Bergenblock, Ringhals AB

CO-SUPERVISOR:

Fredrik Normann, Chalmers University of Technology

EXAMINER

Klas Andersson, Chalmers University of Technology

Department of Energy and Environment

Division of Energy Technology

CHALMERS UNIVERSITY OF TECHNOLOGY

Göteborg, Sweden 2012

Report no. T2012-374

Cooldown capability of Ringhals 3 residual heat removal system
A transient numerical simulation from 4 hours to 36 hours after reactor shutdown
Master's Thesis within the Sustainable Energy Systems programme
JAKOB DOTEVALL
JENNIE NORDKVIST

© JAKOB DOTEVALL, JENNIE NORDKVIST, 2012

Department of Energy and Environment
Division of Energy Technology
Chalmers University of Technology
SE-412 96 Göteborg
Sweden
Telephone: + 46 (0)31-772 1000

Cover:
Schematic layout of a pressurized water reactor including the position of the cooling chain for decay heat.

Chalmers Reproservice
Göteborg, Sweden 2012
Report no. T2012-374

Cooldown capability of Ringhals 3 residual heat removal system

A transient numerical simulation from 4 hours to 36 hours after reactor shutdown

Master's Thesis in the *Sustainable Energy Systems programme*

JAKOB DOTEVALL

JENNIE NORDKVIST

Department of Energy and Environment

Division of Energy Technology

Chalmers University of Technology

ABSTRACT

Stricter requirements on licenses for operating nuclear power plants in Sweden have resulted in a need for more thorough analyses at Ringhals nuclear power plant. At Unit 3, it is of interest to investigate the cooling process after a reactor shutdown to find methods of verifying both the cooldown capability (i.e. cooldown time) and the performance of the heat exchangers involved in this process. Since few other analyses have considered the transient conditions during cooldown, it is important to evaluate how these conditions affect the process. It is also of interest to find out how the cooldown capability is affected by plugged tubes and fouling in the heat exchangers.

The investigation was made by constructing a transient computational model of the cooling chain responsible for removing residual heat from the reactor. The model describes the process of reducing the temperature of the reactor coolant from 177°C to 60°C. The heat transfer capacities for the heat exchangers are evaluated using Kern's method.

The results show that the heat load due to the so-called sensible heat (heat stored in the water and structural material), constitutes 10 to 15% of the total heat load. The sensible heat load is too large to neglect when evaluating the cooldown capability and it is therefore required that the evaluation of the cooling chain includes transient terms. Furthermore, to meet the cooldown time requirement of maximum 36 hours, the required heat transfer capacities of the component cooling and residual heat removal heat exchangers are found to be 1306 kW/°C and 541 kW/°C, respectively. The cooling chain in its current state is over-dimensioned and well capable of meeting its requirements. Plugging of tubes (decreasing the heat transfer area) and fouling (decreasing the heat transfer) in the heat exchangers are not a concern with respect to the cooldown time requirement. However, more measurements to determine the actual fouling values in the heat exchangers are recommended to verify these conclusions.

Keywords:

Nuclear power, Ringhals, cooldown capability, transient simulation, heat exchanger, Kern's method, residual heat removal, sensible heat load

Contents

PREFACE	V
NOTATIONS	VII
1 INTRODUCTION.....	1
1.1 Aim of thesis	1
1.2 Limitations	2
1.3 Method	2
2 TECHNICAL SYSTEM	3
2.1 Pressurized water reactor, PWR.....	3
2.1.1 Shutdown process.....	4
2.2 Cooling chain structure	4
2.2.1 Residual heat removal system, RH-321	5
2.2.2 Component cooling system, CC-711	5
2.2.3 Salt water system, SW-715	6
3 COOLING CHAIN MODEL	7
3.1 Assumptions and input data	7
3.1.1 Flow rates	9
3.1.2 Heat loads	10
3.1.3 Heat exchangers	11
3.1.4 Thermal properties of fluids	12
3.2 Theoretical description of model.....	13
3.3 Simulation procedure	15
3.3.1 Solver algorithm.....	15
3.3.2 Control of flow rate in the residual heat removal system	15
3.3.3 Thermal properties of fluids	15
4 VALIDATION	17
4.1 Comparison with measured data	17
4.2 Comparison with results from the project GREAT	20
4.3 Validation of CC-711 heat exchanger sub-model	21
4.4 Validation of RH-321 heat exchanger sub-model	23
5 RESULTS.....	27
5.1 Simulation results	27
5.2 Sensible heat loads during the cooldown process	30
5.3 Heat exchanger capacity requirements.....	33
5.4 UA-value measurements for the RH-321 heat exchanger.....	35

5.5	Influence of plugged tubes in the heat exchangers	36
5.6	Influence of fouling in the heat exchangers	37
5.7	Limiting components.....	39
5.8	The impact of flow rates on cooldown time.....	40
6	CONCLUSION	41
7	REFERENCES.....	43
	APPENDIX A – DECAY HEAT LOAD.....	I
	APPENDIX B – HEAT CAPACITY RC-313	III
	APPENDIX C – HEAT EXCHANGER THEORY.....	V
	APPENDIX D – AUXILIARY HEAT LOADS ON CC-711.....	IX
	APPENDIX E – MATLAB SCRIPTS	XI
	APPENDIX F – SIMULINK MODEL LAYOUT.....	XV
	APPENDIX G – PERFORMANCE TEST	XIX
	APPENDIX H – SIMULATION RESULTS	XXI

Preface

This report is a result of a Master Thesis project carried out as part of the Master Program in Sustainable Energy Systems at Chalmers University of Technology in Gothenburg. The aim of the thesis work was to investigate the effects of transient conditions during the reactor shutdown process by constructing and performing simulations with a computational model of the cooling chain for decay heat at Ringhals 3. The work was carried out at the nuclear power plant Ringhals at the department RTAT, from January to May 2012.

First of all we want to thank Per-Olof Eklund and Anna Olsson at Ringhals for making this thesis possible. A special thank is also given to Tobias Bergenblock at Ringhals for supervising this thesis, including sharing his valuable knowledge and supporting us. At the department of Energy and Environment at Chalmers University of Technology we want to thank our examiner Klas Andersson and Fredrik Normann for reviews, support and guidance throughout the work process. Finally, we want to thank Mathias Gourdon at Chalmers University of Technology and Rodrik Fällmar and all employees at the department of RTAT at Ringhals for taking your time to discuss and answering all our questions.

Väröbacka, May 2012

Jakob Dotevall

Jennie Nordkvist

Notations

Abbreviations

BWR	Boiling water reactor
CC-711	Component Cooling System
GREAT	Gradual Energy Addition Unit Three
PIS	Process Information System
PWR	Pressurized water reactor
R3	Ringhals Unit 3
RC-313	Reactor Cooling System
RCP	Reactor coolant pump
RH-321	Residual Heat Removal System
SW-715	Salt Water System
UA	Heat transfer capacity

Letters

A	Heat transfer area [m^2]
C	Heat capacitance [$\text{J}/^\circ\text{C}$]
c_p	Specific heat capacity [$\text{J}/\text{kg}^\circ\text{C}$]
F_t	Temperature correction factor
k_f	Thermal conductivity [$\text{W}/\text{m}^2\text{C}$]
Q	Heat load [W]
T	Temperature [$^\circ\text{C}$]
U	Overall heat transfer coefficient [$\text{W}/\text{m}^2\text{C}$]
\dot{m}	Mass flow rate [kg/s]
ρ	Density [kg/m^3]
μ	Viscosity [$\text{Pa}\cdot\text{s}$]

Subscripts

CC	Component cooling
CCAUX	Component cooling auxiliary
CCR	Component cooling return
CCRH	Component cooling residual heat
RC	Reactor cooling
RCP	Reactor coolant pump
RH	Residual heat
SENS	Sensible
SW	Sea water
SWR	Sea water return

1 Introduction

Ringhals nuclear power plant is located on the Swedish west coast in the county of Varberg. The plant is the largest power plant in Scandinavia with an electricity production of 28 TWh/year which corresponds to approximately 20% of the annual Swedish electricity production. Ringhals has four reactors, one boiling water reactor (BWR) and three pressurized water reactors (PWRs) with a total installed capacity of 3702 MW. Ringhals AB is owned by Vattenfall AB (70.4%) and E.ON (29.6%) [1].

Nuclear power plants are continuously validated to ensure reliability and absence of defects. The Swedish Radiation Safety Authority has in the recent years introduced more stringent requirements to get an operating license. These stringencies have influenced the requirements of performing operability verification tests of safety systems and components. The verification work needs to include investigations on system level as well as on component level. It is important to find limiting factors (process parameters) and analyse what impact they have in various operating conditions.

At Ringhals Unit 3, these increased safety requirements have resulted in a need for better methods to verify the performance of the heat exchangers in the residual heat removal system and the component cooling system. These two systems, together with a salt water system, constitute the cooling chain for decay heat from nuclear fuel. Decay heat is the heat released due to radioactive decay in the reactor core, and the removal of this heat is an important part of the reactor shutdown process.

The challenge of verifying operability of the heat exchangers is twofold. Firstly, a heat exchanger requirement that satisfy the system requirements should be determined in terms of heat transfer capacity. Secondly, it must be verified that this heat exchanger capacity is actually fulfilled, a verification associated with several difficulties. One of the main problems is that the heat exchangers are dimensioned for high heat loads, at operating conditions such as during a reactor shutdown process. During normal operation the heat loads are much smaller, and with these loads it is hard to estimate the correct capacity of a heat exchanger due to measurement uncertainties. Under normal circumstances the reactor is only shut down once a year, which means that high loads are rare.

Since high heat loads are not achieved during normal operation, an alternative to measurements is required. One possibility is to simulate the process numerically with a computer model. Simulations could then be used to obtain information on the behaviour of the heat exchangers during different operational conditions, which is important when trying to find more accurate methods to verify heat exchanger performance. Because of the transient conditions and dynamic relations between the interconnected systems, the complete cooling chain needs to be included in the computational model. Since most of the previous analyses involving the cooling chain at Ringhals 3 are steady-state (i.e. time independent), the effects of the transient conditions during a reactor shutdown process are not well known. It is of interest to study the importance of these effects, since it is possible they may affect the way some safety functions are verified.

1.1 Aim of thesis

The aim of this thesis is to investigate the effects of transient heat loads during the reactor shutdown process by constructing a computational model of the cooling chain for decay heat.

The transient heat loads due to decay and sensible heat will be evaluated, and the cooldown capability (i.e. cooldown time) analysed. It will also be determined if transient calculations are necessary for validating heat exchanger performance and cooldown capability, or if steady-state analyses are sufficient.

The heat transfer capacities of the heat exchangers in the cooling chain during the reactor shutdown process will be studied, and capacity requirements necessary to meet the requirement on the cooling chain will be suggested. Furthermore, it will be studied how plugged tubes and fouling in the heat exchangers affect the cooldown capability.

In addition, the limiting components in the cooling chain will be identified.

1.2 Limitations

To limit this thesis work three important boundaries are set:

- Only the cooling chain at Ringhals 3 is investigated in this thesis. Although the cooling chain at Ringhals 4 is similar, conclusions drawn in this report may not necessarily apply to both units.
- Two cases are simulated; reactor cooldown during normal conditions and during accidental conditions (where several components are unavailable). No other cases, like plant start-up and recirculation, are investigated.
- The components in the cooling chain affected by component requirements are heat exchangers and pumps. Since the requirements and verification methods of pumps are well known, only the heat exchangers are investigated.

1.3 Method

The investigation is based on simulations of the reactor cooldown process. These simulations were enabled by the construction of a transient computational model, which was part of the thesis work. The model is based on information specified in reports and flow charts of the Ringhals 3 cooling system in combination with mathematical theory describing transient cooling processes. The transient computer model is implemented in the MathWorks Simulink software. Simulink was chosen due to its capability of handling the transient process and dynamic conditions in the cooling chain.

The hazardous nature of nuclear power requires that calculations associated with nuclear safety must have a safety margin. This safety margin was added in the computational model through the use of *conservatism*, which means that assumptions and estimations for input data are made to underestimate the plant performance. Using conservative assumptions is the general way of working in the nuclear business today.

The constructed computational model was validated by comparing simulation results with both measurement data and results from a comparable project [2]. Furthermore, each sub-model was validated separately. Finally the model was used to simulate the cooldown process at Ringhals 3. The results from the simulations were analysed in order to increase the knowledge about effects due to transient conditions in the cooling chain. Further, sensitivity analysis for the system was conducted by parameter studies.

2 Technical system

This chapter describes the three interconnected systems in the cooling chain, along with a general description of the main process.

2.1 Pressurized water reactor, PWR

Ringhals Unit 3 (R3) is a pressurized water reactor (PWR). In a PWR, the process is separated into a primary and a secondary system. A schematic picture of the main process can be seen in Figure 2.1. The primary system comprises the reactor cooling circuit and the secondary system comprises the path from the steam generators through the turbines and the condenser and back through the feed water system. At R3 there are three reactor cooling circuits with one steam generator per circuit. Note that only one of the reactor cooling circuits is included in Figure 2.1.

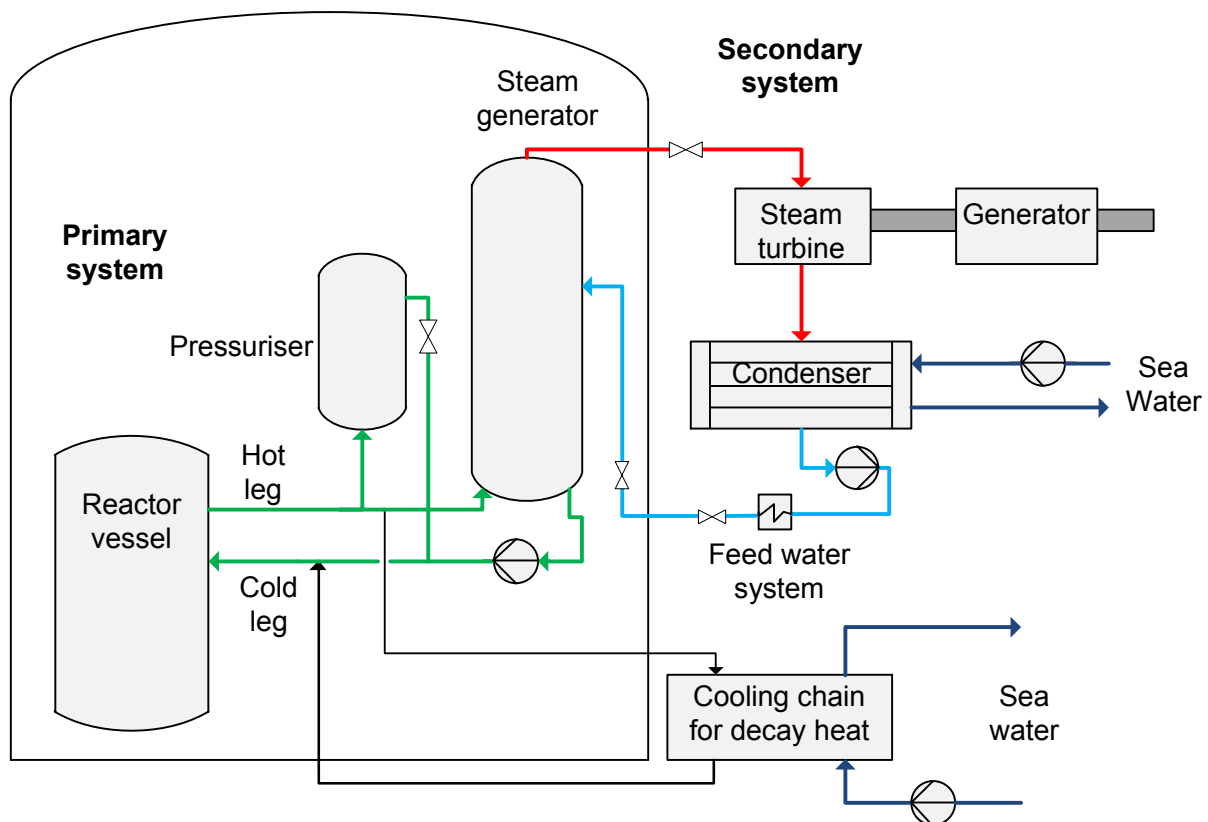


Figure 2.1 – Flow chart describing the main process in a PWR [3].

The reactor core, which mainly consists of the nuclear fuel, is located in the reactor vessel. Due to nuclear reactions in the fuel, heat is generated. The heat is transported to the steam generators by the water in the primary system. This water, called reactor coolant, comes into the reactor vessel through the “cold leg” at a temperature of around 285°C and is heated to 320°C when passing through the reactor core. Due to a high pressure of around 154 bars, no boiling takes place. The heated reactor coolant flows through the “hot leg” to the steam generator where heat is transferred from the primary to the secondary system. In the secondary system feed water with lower pressure is evaporated. The reactor coolant is pumped back through the “cold leg” to the reactor vessel, while the steam is lead to the

turbines. Here it is expanded, forcing the turbine to rotate and create shaft work which is converted into electric energy by the generator. After the turbine, the steam is condensed in the condenser and pumped through the pre-heaters and the feed water system back to the steam generators [4].

2.1.1 Shutdown process

The reactor shutdown process is the process of reducing the temperature of the reactor coolant from 320°C to below 60°C. It also includes a reduction in pressure from 154 bars to atmospheric pressure. The shutdown is initiated by inserting control rods into the reactor core. These control rods stop the nuclear chain reactions, which is responsible for the major part of the heat generation during normal operation. However, decay heat from the radioactive decay is still generated and must be removed. During the first part of the cooldown process, heat is transferred to the secondary system via the steam generators and cooled away. During the second part, which is below 177°C and 29 bars, the cooling is done by the cooling chain for decay heat.

2.2 Cooling chain structure

The cooling chain investigated in this thesis consists of three systems, the residual heat removal system (RH-321), the component cooling water system (CC-711) and the salt water system (SW-715). The residual heat removal system is interconnected to the component cooling system through the RH-321 heat exchangers. Furthermore, the component cooling system is also interconnected to the salt water system through the CC-711 heat exchangers. Figure 2.2 shows an overview of one of the trains in the cooling chain. Two identical trains are connected in the reactor cooling system.

The main purpose of the cooling chain is to remove residual heat from the reactor core. The residual heat consists of both decay heat and heat stored in water and structural materials in the reactor cooling system. As mentioned above, the cooling chain is designed to be able to bring the reactor coolant temperature down to below 60°C. During so called accidental conditions, when one of the trains is unavailable, the reactor coolant temperature must be reduced below 100°C within 36 hours after shutdown initiation. This requirement must be fulfilled at all times.

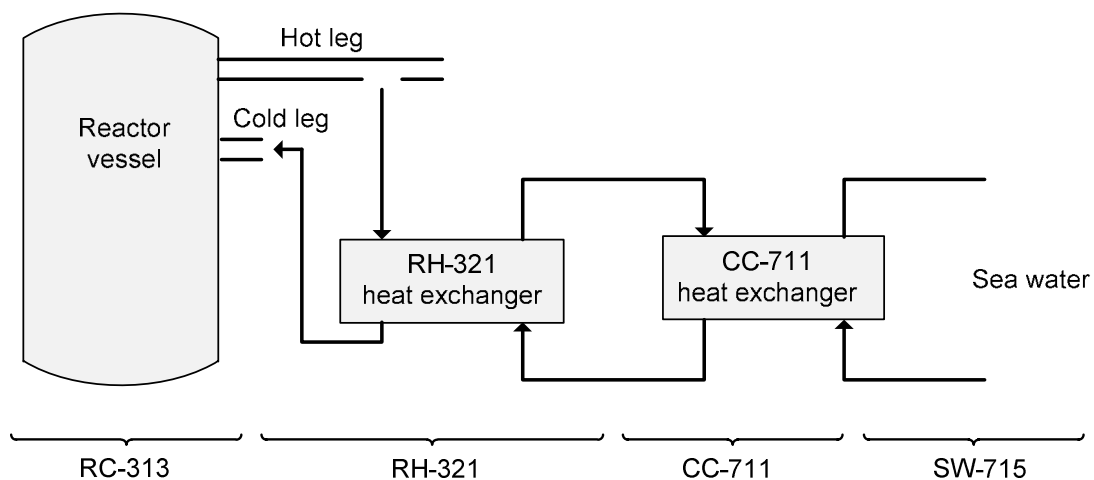


Figure 2.2 - Schematic picture of one of the train in the cooling chain.

2.2.1 Residual heat removal system, RH-321

The residual heat removal system has two primary functions. The first is to remove residual heat from the reactor cooling system (RC-313) during normal cooldown. The second is to operate as the low pressure emergency cooling system in case of an accident. The residual heat removal system becomes operational when the pressure and temperature in the reactor cooling system is below 29 bars and 177°C, which corresponds to the second phase of a reactor shutdown. The residual heat removal system is divided into two redundant trains, the A- and B-side. Each train consist of a pump, a heat exchanger, a pneumatics control valve, a bypass valve and motor operated shutoff valves.

During normal cooldown water from the hot leg flows through the motor operated shutoff valve to the residual heat exchangers. The flow through each residual heat exchanger is controlled by two valves, a pneumatics control valve and a bypass valve. Figure 2.3 gives a schematic picture of the system. The pneumatics control valve opens when cooling is desired and the bypass valve regulates the circuit total flow so it is held constant. When no cooling is desired, the total stream flows through the bypass valve. Thereafter, water flow to the cold leg of the reactor cooling system and back into the reactor vessel [5]. Regulating the flow ratio between the bypass and the heat exchanger is the main way for the reactor operators to control the cooldown rate.

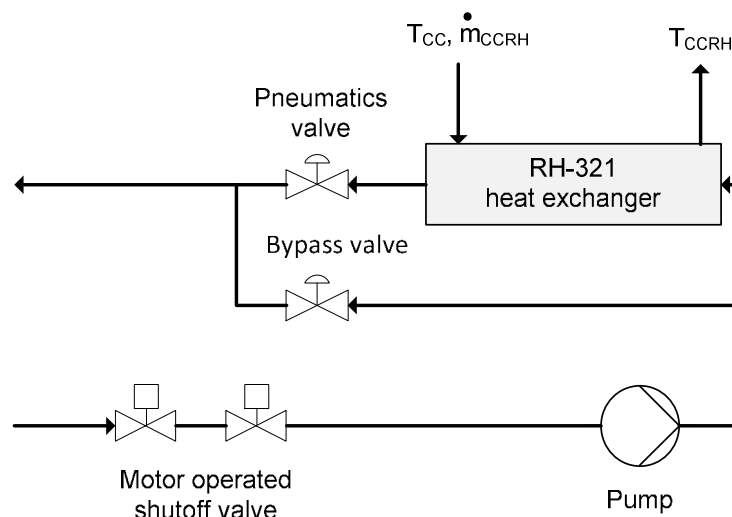


Figure 2.3 – Schematic picture of water flow in RH-321 circuit during normal cooldown [5].

2.2.2 Component cooling system, CC-711

The component cooling system has two main functions where the primary function is to provide cooling water to components for heat removal. Its secondary function is to act as a barrier between the residual heat removal system and the salt water system i.e. prevent leakage of radioactive particles into the environment. The latter is achieved since the component cooling system is a closed system, which can be seen in Figure 2.2.

To ensure cooling capacity in case of accidents, the component cooling system is divided into two redundant trains, the A- and B-side. Each train has two parallel pumps and consists of a low and a high temperature part with one heat exchanger in each. Both trains include safety and non-safety related objectives [6]. The safety related components that receives cooling

from the high temperature part are two residual heat removal heat exchangers (RH-321 heat exchangers), two sprinkler heat exchangers and one spent fuel heat exchanger. In addition to this some other non-safety components are cooled by the high temperature part. The low temperature part cools different safety related pumps and other various components in the plant that needs lower flow temperature.

2.2.3 Salt water system, SW-715

The salt water system supplies the component cooling system with sea water cooling. The system consists of two redundant trains, A- and B-side. Each train supply cooling water to both a low and a high temperature component cooling heat exchanger. Each train also has a mussel filter system, a tube cleaning system and two parallel pumps. After passing through the heat exchangers, the sea water ends up in a cascade pool before being led back to the sea [7].

3 Cooling chain model

This chapter presents the developed cooling chain model and how it is used in this thesis. The assumptions made and input data used are first presented, followed by a theoretical description of the model. Finally the simulation procedure is described.

The model is used to simulate the later part of the transient cooling process after a reactor shutdown, i.e. the process of decreasing the reactor coolant temperature from 177°C to 60°C. This part of the cooling process takes place in the cooling chain described in Section 2.2. Two cases are studied:

- Case 1: Normal conditions. One RH-321 train operates when T_{RC} is between 177°C – 120°C, both trains operates when T_{RC} is below 120°C. No requirement in terms of cooldown time.
- Case 2: Accidental conditions. One RH-321 train unavailable, the cooling process is undertaken with only one train in operation. Requirement: T_{RC} to be decreased below 100°C within 36 hours.

Due to differences between the Swedish and the American definition of a “cold shutdown”, 93°C is sometimes used instead of 100°C. Since the Swedish Radiation Safety Authority’s definition of a cold shutdown is based on 100°C, this number is used in this work.

Since the low temperature part of component cooling system does not affect the residual heat removal, only the high temperature part is included. Also note that in Case 1 both CC-711 trains are in operation while only one is in operation in Case 2.

3.1 Assumptions and input data

Residual heat removal is initiated when the reactor coolant temperature is 177°C, which is considered to be four hours after reactor shutdown. At this temperature, the steam generators starts to be inefficient and therefore the heat transferred from the reactor cooling system to the steam generators is considered negligible. Also, the reactor vessel and all pipes are well isolated, and therefore the thermal losses within the reactor cooling system is considered equal to the heat input from residual heat removal pumps (around 300 kW).

The heat removed by the residual heat removal system consists of:

- Decay heat from the reactor core.
- Heat stored in the reactor cooling system, so called sensible heat.
- Reactor coolant pumps.

This heat is transferred to the component cooling system via the RH-321 heat exchangers. The component cooling system is warmed by:

- Heat from the residual heat removal system (via the RH-321 heat exchangers).
- Auxiliary heat loads cooled by the component cooling system.

- CC-711 pumps.

The CC-711 heat exchangers transfer the heat to the salt water system, which has the following heat loads:

- Heat from the component cooling system (via the CC-711 heat exchangers).
- SW-715 pumps. These are included in the heat balance since they are located upstream of the CC-711 heat exchangers.

The two trains and their components are considered to be identical.

There are also some other constraints on the cooling chain. The absolute temperature gradient in the reactor cooling system, dT_{RC}/dt , must not exceed $28^{\circ}\text{C}/\text{h}$ to avoid high levels of thermal stress. The temperature after the CC-711 heat exchanger must be lower than 48.9°C since higher temperatures could damage sensitive components. Finally, to avoid boiling, the outlet temperature on the cold side of the RH-312 heat exchanger, T_{CCRH} , should not exceed 80°C .

Table 3.1 below summarizes the most important input data used within the simulations. Note that only one train is in operation in Case 2. Some of the input data are described in more detailed in Section 3.1.1-3.1.4.

Table 3.1 - Summary of input data used in simulations.

Input data	Value	Reference
Initial conditions		
RC-313 temperature, T_{RC}	177°C	
Time cooldown initiated	4 h	
Heat loads		
Decay heat load	See Appendix A	[8] – see Section 3.1.2
Auxiliary heat load at 4 hours	8.275 MW	[9] – see Section 3.1.2
Auxiliary heat load at 20 hours	1.975 MW	[9] – see Section 3.1.2
RC-313 pumps	4.4 MW/pump	[10]
CC-711 pumps	0.160 MW/pump	[9]
SW-715 pumps	0.200 MW/pump	[9]
RC-313		
RC heat capacity	3415 MJ/°C	[10] – see Section 3.1.2
Maximum temperature gradient RC	28°C/h	[11]
RC pumps in operation	1	[11]
RC pumps stop temperature	70°C	[11]
RH-321		
Number of RH heat exchangers in operation	1 ($T_{RC} \geq 120^\circ\text{C}$) / 2 ($T_{RC} < 120^\circ\text{C}$)	[11]
CC-711		
Maximum T_{CCRH}	80°C	
Maximum T_{CC}	48.9°C	[10]
Number of CC heat exchangers in operation	2	[11]
CC pumps in operation	4 (2 per train)	[9]
SW-715		
SW temperature, T_{SW}	25°C	
SW pumps in operation	2 / 4 (1 / 2 per train)	See Section 3.1.1

3.1.1 Flow rates

The flow rate in the residual heat removal system must be controlled in order to not exceed the temperature gradient limit of the reactor cooling system. In the salt water system two pumps per train are assumed to be in operation during the first stage of the cooldown ($T_{RC} \geq$

120°C) to avoid too high temperatures in component cooling system [11]. A summary of the flow rates can be found in Table 3.2.

Table 3.2 – Flow rates used in simulations.

Input data	Value	Reference
RH flow rate per heat exchanger	≤ 234.36 kg/s	[10]
CC flow rate per RH heat exchanger	252 kg/s	[10]
CC flow rate per CC heat exchanger	504 kg/s	[10]
SW flow rate per heat exchanger	720 kg/s (two pumps/train)	[10]
	420 kg/s (one pump/train)	

3.1.2 Heat loads

The purpose of the cooling chain is to remove heat from several sources. The heat sources included in the model are decay heat from the reactor core, heat stored in the reactor coolant system, heat from auxiliary loads in the component cooling system and heat input from pumps.

The decay heat is the heat released as a result of radioactive decay. The heat generation after a reactor shutdown decreases over time, and is presented in a decay heat table. The decay heat table used in this study assumes a 12 month fuel cycle and considers fission products, actinides contribution as well as contributions from activated structural materials. The decay heat table is given in Appendix A.

Heat stored in fluids and structural materials, so called sensible heat, also contributes to the overall cooling demand. In the reactor coolant system the lumped-capacitance method is used to consider the stored heat. This implies that the reactor cooling water, the secondary water in the steam generators and the steel are in thermal equilibrium and that the temperature is spatially uniform at any instant during the process [12]. The sensible heat is represented by the heat capacity which is the thermal energy that must be extracted from the reactor cooling system to reduce the temperature by 1°C. In this model, a standard value of 3415 MJ/K is used for the reactor cooling system. It is denoted as C_{RC} , and is based on the characteristics of a nuclear plant similar to Ringhals 3. For details see Appendix B. Due to the low temperatures and the comparably low heat capacities in the component cooling system and the salt water system, the stored heat in these systems is considered negligible.

In the component cooling system there are a number of other heat sources, referred to as auxiliary heat loads. These sources are grouped together in the model and simulated as one heat load, Q_{CCAUX} . As mentioned above, only heat sources in the high temperature part of the component cooling system is included.

Data for Q_{CCAUX} are only available at 4 hours and 20 hours after reactor shutdown, see Appendix D. The load is assumed to decrease linearly between these two points, and after 20 hours remain constant. Also, it is assumed that the load is equally distributed between the two CC-711 trains.

The net heat input from the component cooling pumps is included in Q_{CCAUX} , and is considered to be constant over time. In this study a value of 0.155 MW per pump is used (two component cooling pumps per train) which corresponds to a component cooling flow rate of 504 kg/s per train [13]. In Case 1 there are always two CC-711 trains in operation, i.e. the total net heat input from component cooling pumps is 0.62 MW. In Case 2, where one train is unavailable, the corresponding value is 0.31 MW.

3.1.3 Heat exchangers

The heat transfer capacity, UA , for the heat exchangers is calculated by using Kern's method, an empirically based method. The method is described in Appendix C. There are some assumptions and simplifications adapted in the calculations related to Kern's method. It is assumed that the flows are fully turbulent and that there are no difference in fluid viscosity between wall and bulk. When calculating the inside heat transfer coefficient of the tubes for the RH-321 heat exchangers, the simplified equation used for natural water is considered to be valid for reactor cooling water. In the same heat exchanger, the hypothetical cross-flow area on the shell-side is estimated from the flow velocity in the design point given by the manufacturer. Furthermore, it is not taken into account that the physical properties of the fluids vary inside the heat exchangers. The properties are given for average temperatures over the heat exchangers.

The pressure drop in the heat exchangers is not accounted for in the model. Physical properties are taken at design operating pressures, except for the reactor cooling water where properties are taken at 27 bars (corresponding to the pressure at cooldown initiation). Fouling of the heat transfer surfaces is assumed to not differ between tubes. In the CC-711 heat exchanger the baffle spacing varies, and an average value is used.

The design fouling factors are specified by the manufacturer, and are defined as the highest allowable fouling factors for the heat exchangers to meet the heat transfer capacity stated in the specification. The design fouling factor is used in the simulations if nothing else is specified.

A summary of the data inputs can be seen in Table 3.3.

Table 3.3 – Design data used in the model for the heat exchangers [14, 15, 16, 17].

	CC-711 heat exchanger	RH-321 heat exchanger
Type of heat exchanger	Tube and shell	U-tube and shell
Fluid on tube-side	Sea water	Reactor cooling water
Fluid on shell-side	Component cooling water	Component cooling water
Operating pressure tube/shell [bars]	3.1 / 7	27 / 11.3
Number of tubes	2442	415
Tube length [mm]	7162	5580
Tube arrangement	Triangular	Triangular
Baffle spacing [m]	0.387	0.44
Design flow velocity shell-side [m/s]	n/a	1.75
Thermal conductivity tube material [W/m°C]	16.4 (Ti Gr.2)	16 (SA 249 TP304)
Design fouling shell side [m ² °C/W]	$8.8 \cdot 10^{-5}$	$9 \cdot 10^{-5}$
Design fouling tube side [m ² °C/W]	$8.8 \cdot 10^{-5}$	$5 \cdot 10^{-5}$
Number of plugged tubes	0	0

3.1.4 Thermal properties of fluids

The physical properties used in the simulations are listed in Table 3.4. The properties are varied with temperature, with the exception of the specific heat capacity for the component cooling water. This value does not vary much with temperature, and therefore a constant value is taken at 25°C. For sea water, the properties are based on a salinity of 35 g/kg water.

The process fluid in the residual heat removal system is borated water (3-4% boric acid). A sensitivity analysis was carried out to see how the physical properties changed with the amount of boron in the water. It was concluded that the differences are small and negligible when the boron content is low (3-4%), and therefore fluid properties for ordinary water was used.

Table 3.4 – Physical properties of the fluids included in the cooling chain [18, 19].

Property	SW-715	CC-711	RH-321
Specific heat capacity, c_p [J/kg°C]	4001.3 (at 25°C) - 4015.0 (at 60°C)	4182.9	4177.9 (at 60°C) - 4397.9 (at 180°C)
Density, ρ [kg/m ³]	1023.6 (at 25°C) - 1009.0 (at 60°C)	n/a	984.3 (at 60°C) - 888.1 (at 180°C)
Thermal conductivity, k_f [W/m°C]	0.6087 (at 25°C) - 0.6485 (at 60°C)	0.6078 (at 25°C) - 0.6638 (at 75°C)	n/a
Viscosity, μ [Pa·s]	0.00095 (at 25°C) - 0.00050 (at 60°C)	0.00089 (at 25°C) - 0.00037 (at 75°C)	n/a

3.2 Theoretical description of model

The model is based on a number of relations describing the heat transfer process from heat source to heat sink. The notations used in the equations are given in Figure 3.1.

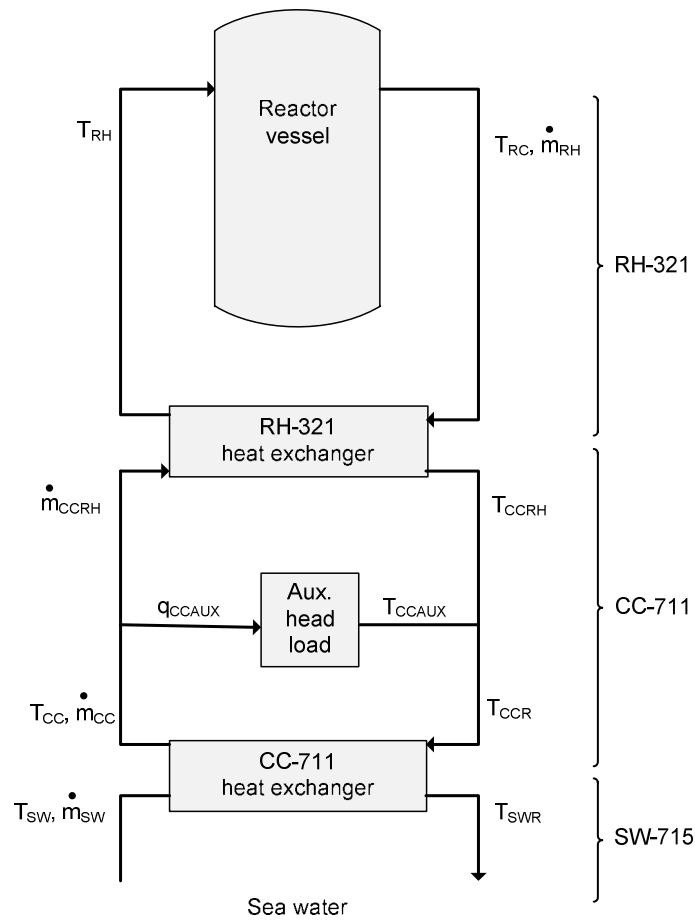


Figure 3.1 – Flow chart with notations. The same notations are used in the equations.

Equation 1 is based on the first law of thermodynamics and describes the heat balance over the reactor cooling- and residual heat removal systems. It is applied to a control volume including the reactor and the pipes in the reactor cooling and residual heat removal systems. The sensible heat load is equal to the pump and decay heat generation minus the heat transferred to the component cooling system via the RH-321 heat exchangers:

$$C_{RC} \frac{dT_{RC}}{dt} = Q_{RC}(t) + Q_{RCP}(t) - Q_{RH}(t) \quad (1)$$

Note that T_{RC} decreases over time, i.e. the time derivative is negative.

Equations 2 to 4 describe the heat transferred in the RH-321 heat exchanger. Equation 2 is a general relation for heat transfer across a surface. Since the heat exchanger has two tube passes the flow is not true counter-current, therefore a temperature correction factor F_T must be included [20]:

$$Q_{RH} = UA_{RH} F_T \frac{(T_{RH} - T_{CC}) - (T_{RC} - T_{CCRH})}{\ln \frac{T_{RH} - T_{CC}}{T_{RC} - T_{CCRH}}} \quad (2)$$

The heat transferred can also be expressed as heat balance over each side of the heat exchanger:

$$Q_{RH} = \dot{m}_{RH} c_{P,RH} (T_{RC} - T_{RH}) \quad (3)$$

$$Q_{RH} = \dot{m}_{CCRH} c_{P,CC} (T_{CCRH} - T_{CC}) \quad (4)$$

The heat transferred in the CC-711 heat exchanger is described by Equations 5 to 7, corresponding to those used for the RH-321 heat exchanger. In this case the heat exchanger is one-pass and the flow is true counter-current, i.e. the temperature correction factor can be excluded:

$$Q_{CC} = UA_{CC} \frac{(T_{CC} - T_{SW}) - (T_{CCR} - T_{SWR})}{\ln \frac{T_{CC} - T_{SW}}{T_{CCR} - T_{SWR}}} \quad (5)$$

$$Q_{CC} = \dot{m}_{CC} c_{P,CC} (T_{CCR} - T_{CC}) \quad (6)$$

$$Q_{CC} = \dot{m}_{SW} c_{P,SW} (T_{SWR} - T_{SW}) \quad (7)$$

Equations 8 to 10 are linked to the auxiliary heat loads in the component cooling system. The flow rate through the CC-711 heat exchanger is equal to the sum of the flow rates through the RH-321 heat exchanger and through the auxiliary components:

$$\dot{m}_{CC} = \dot{m}_{CCRH} + \dot{m}_{CCAUX} \quad (8)$$

The return temperature to the CC-711 heat exchanger is expressed by a heat balance over the mixing point where the two streams converge:

$$\dot{m}_{CC}T_{CCR} = \dot{m}_{CCAUX}T_{CCAUX} + \dot{m}_{CCRH}T_{CCRH} \quad (9)$$

The temperature after the auxiliary heat loads is calculated using a heat balance over the auxiliary components:

$$T_{CCAUX} = T_{CC} + \frac{Q_{CCAUX}}{\dot{m}_{CCAUX}c_{p,CC}} \quad (10)$$

3.3 Simulation procedure

The computational model uses the input data, initial guesses and the relations presented in Sections 3.1-3.2 to calculate temperatures in the cooling chain at every time step during the simulation. The model uses a variable time step size of maximum 200 s/step. All inputs are controlled through a MATLAB-script (see Appendix E).

The two trains are modeled by duplicating Equations 2 to 10. The output from Equation 1, T_{RC} , is used as input to both train A and B. The heat transferred in each RH-321 heat exchanger, $P_{RH,A}$ and $P_{RH,B}$ is added together and used as input in Equation 1. For detailed layouts of the Simulink model, see Appendix F.

3.3.1 Solver algorithm

Equation 1 is an ordinary differential equation (ODE) while the other equations are differential algebraic equations (DAE's). The model uses the built-in ode45 solver to find a solution in every time step. This is an explicit, continuous variable-step solver that uses the Runge-Kutta method to solve ordinary differential equations.

Each DAE implies an algebraic constraint in the model. In Simulink, algebraic constraints are called "algebraic loops" and are solved numerically at every time step by an algebraic loop solver. The definition of an algebraic loop is when an input to a block directly depends on the block's output. To avoid a large and complex loop that the algebraic loop solver can't solve, a memory block is placed in the model. This block outputs the input from the previous time step, which effectively breaks the algebraic loop into two smaller, solvable loops. By using a small time step and a good initial guess, the use of a memory block will have no significant effect on the solution.

3.3.2 Control of flow rate in the residual heat removal system

The flow rates on the hot side of the RH-321 heat exchangers must be limited in order to meet the requirements in system. The outlet temperature on the cold side of the heat exchanger, T_{CCRH} , must not exceed 80°C and the temperature gradient during cooling in the reactor cooling system must be smaller than 28°C/h. In the model these requirements are met by finding the highest allowable flow rate in every time step. The outlet temperature and gradient is tested for flow rates equal to or lower than the design flow rate (234.36 kg/s), and the highest flow rate that satisfies the requirement is used in that time step. This is done for both RH-321 trains.

3.3.3 Thermal properties of fluids

Some of the thermal properties of the process fluids vary with temperature. These are modelled using an Embedded MATLAB Function with temperature as the input and the

corresponding value for the thermal property as the output. The MATLAB function is constructed as table with thermal property values for a range of temperatures, using interpolation for intermediate temperatures.

4 Validation

To validate the computational model, simulation results are compared to measured data from the plant. A comparison is also made with results from a similar evaluation of the cooling chain that was performed within the scope of the GREAT project¹ [2].

Because of the importance of the CC-711 and RH-321 heat exchangers for the cooldown capability, additional validation of the heat exchanger sub-models is performed. These sub-models calculate the heat transfer capacity (UA-value), and the validation is performed by comparing results from the sub-models with performance tests and with the heat exchanger specifications. A specification is written by the heat exchanger manufacturer, and includes the UA-value for a specific combination of temperatures and flow rates. This combination corresponds to the components design point.

4.1 Comparison with measured data

One of the main difficulties with validating the simulated cooldown process is that the plant (during normal circumstances) is only shut down once a year. Since the cooling chain at Ringhals 3 was updated a few years ago, the number of shutdowns available for comparison is limited. Also, the process is affected by a large number of factors making every shutdown process unique. These factors include for example sea water temperature, steam generator performance and operation procedure (number of pumps in operation, control of valves etc.).

However, evaluated measured data show some important similarities when compared with simulation results. Figure 4.1 shows the reactor coolant temperature during shutdowns between 2009 and 2011 along with the same temperature during simulation. When studying Figure 4.1 it is important to consider which parameters that differ between the simulation and the measured data, and how they affect the appearance of the temperature curves. The most obvious difference is that the temperature for the measured data is constant in some intervals. This depends on the fact that the reactor operators can control the temperature by regulating the reactor coolant flow to the RH-321 heat exchangers, and at some points choose to hold the temperature constant. This type of operation can be made for various reasons, but is not included in the model.

¹ This project was carried out between 2004 and 2010 and resulted in increased power output of Ringhals 3 (the name GREAT is an abbreviation for “Gradual Energy Addition unit Three”).

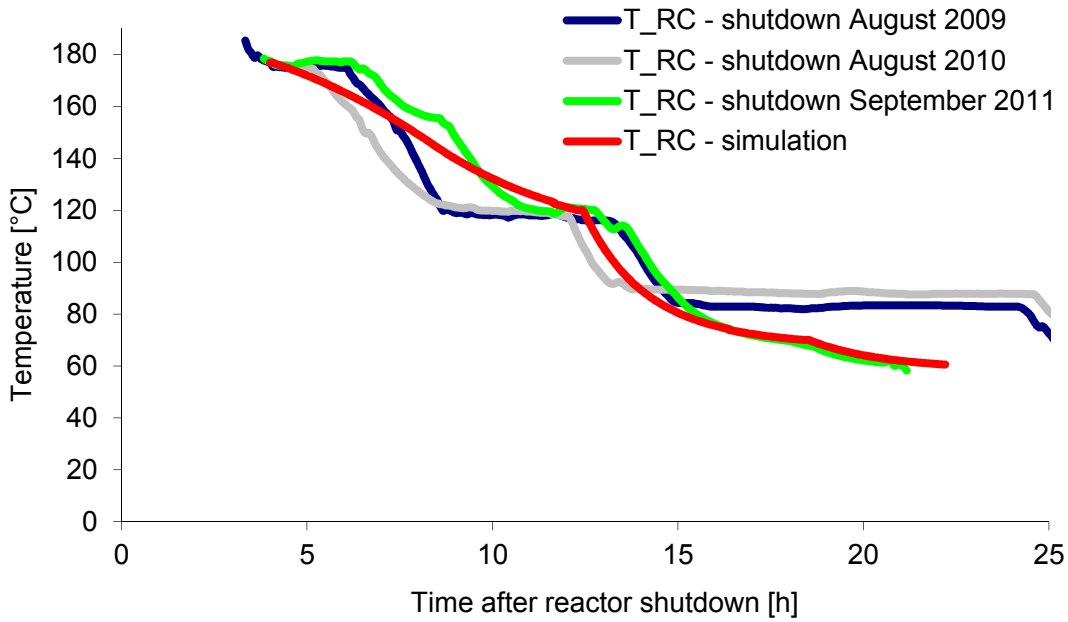


Figure 4.1 - The reactor coolant temperature (T_{RC}) during the cooldown process. Simulated temperature is compared with measured temperatures during the reactor shutdowns 2009 - 2011.

A number of other factors also affect the curves, some of which are presented in Table 4.1. Steam generators are considered to be inefficient in the model, but in the reality they continue to contribute to the cooling process even after the residual heat removal system is placed in operation. The sea water temperature is set to 25°C, which is the most common design sea water temperature in calculations carried out at Ringhals. This temperature has a large effect on the cooldown capability, which will be shown in Section 5.1. The number of reactor coolant pumps (RCP's) in operation is decided by the reactor operator. At least one has to be in operation until T_{RC} is 70°C [21], but during the shutdown 2009 to 2011 all three were in operation. Since the heat input is 4.4 MW per pump, this difference has a high impact on the cooling demand. Another parameter decided by the operator is the flow rates in the systems. Design flow rates (which can be seen as the highest allowable) is used in the model, but during the shutdowns some measured flow rates were slightly lower.

Table 4.1 – Example on differences between measured data and simulation which all affects the appearance of the curves.

	Shutdown August 2009	Shutdown August 2010	Shutdown September 2011	Simulation
Steam generators ineffective?	No	No	No	Yes
Sea water temperature	18.0°C	16.9°C	16.5°C	25°C
Number of RCP's in operation	3	3	3	1 (stopped when $T_{RC} = 70^{\circ}\text{C}$)

One parameter which is complicated to estimate is the fouling of the heat transfer surfaces in the heat exchangers, which affect the heat transfer capacities (see Section 5.6 for a deeper analysis). Fouling values given in the heat exchanger specifications are used in the simulation. These values are the highest allowable and are with most certainty higher than in reality, which will be discussed in Section 4.3. The UA-values are thus underestimated, which can partly explain the larger gradients of the measured temperature curves.

There are also similarities to be seen in Figure 4.1. One clear similarity between all curves can be seen at 120°C. The temperature gradient increases strongly and this is due to the start-up of a second train which increases the cooling capacity. When comparing the simulation curve and the curve for 2011 it can be seen that the cooling capacity decreases at lower temperatures, characterized by a smaller gradient. This is due to lower temperature differences in the cooling chain.

Figure 4.2 shows the temperatures in train A as a function of time during the shutdown 2011. The corresponding temperature curves from the simulation, with the exception of the T_{RH^*} curve, are given in Figure 4.3. T_{RH^*} is the temperature before the RH-321 heat exchanger and it is included to show the process of warming the RH-321 circuit. When T_{RH^*} is close to T_{RC} , the cooling process is initiated and the RH-321 heat exchanger is placed in operation. In the measured data this occurs at around 155°C (indicated in Figure 4.2 by a vertical dashed line), which means that cooling before this point is made by the steam generators only. In the simulation the cooling process is initiated at 177°C, and the RH-321 circuit is assumed to be warmed before the simulation starts. Therefore, when making comparisons, it should be noted that only the right hand of Figure 4.2 can be compared to the curves in Figure 4.3.

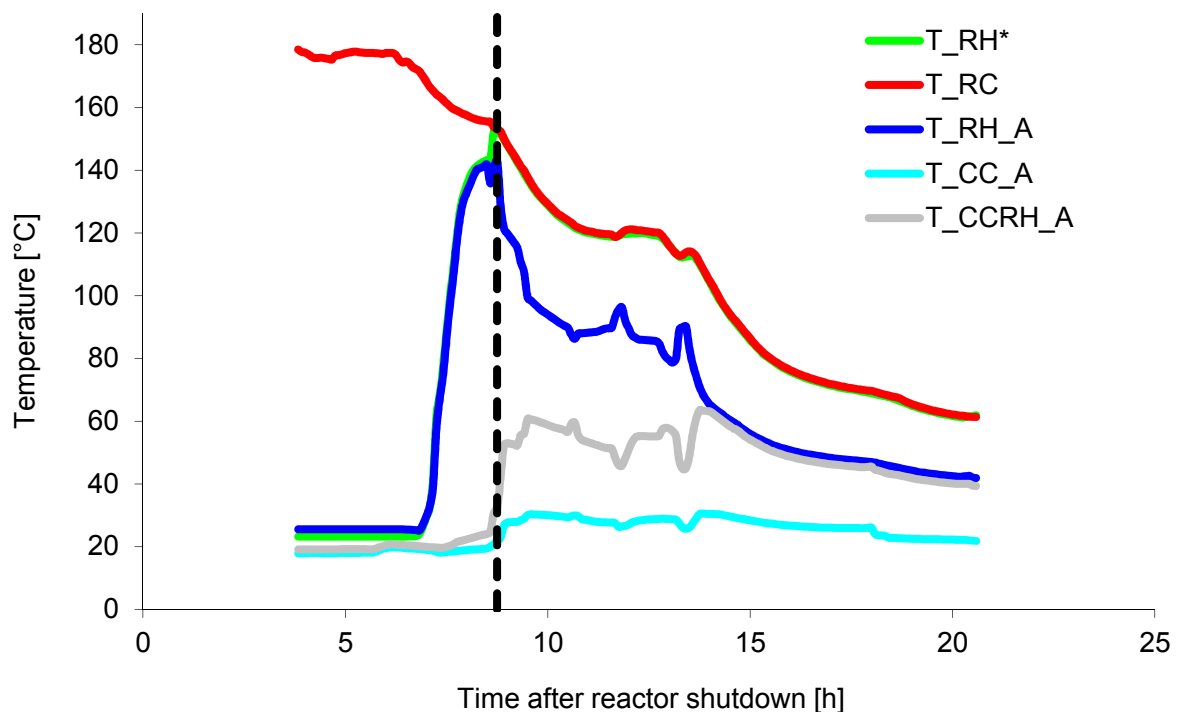


Figure 4.2 – Measured temperatures in train A during shutdown 2011. The vertical dashed line indicates when the cooling chain is placed in operation.

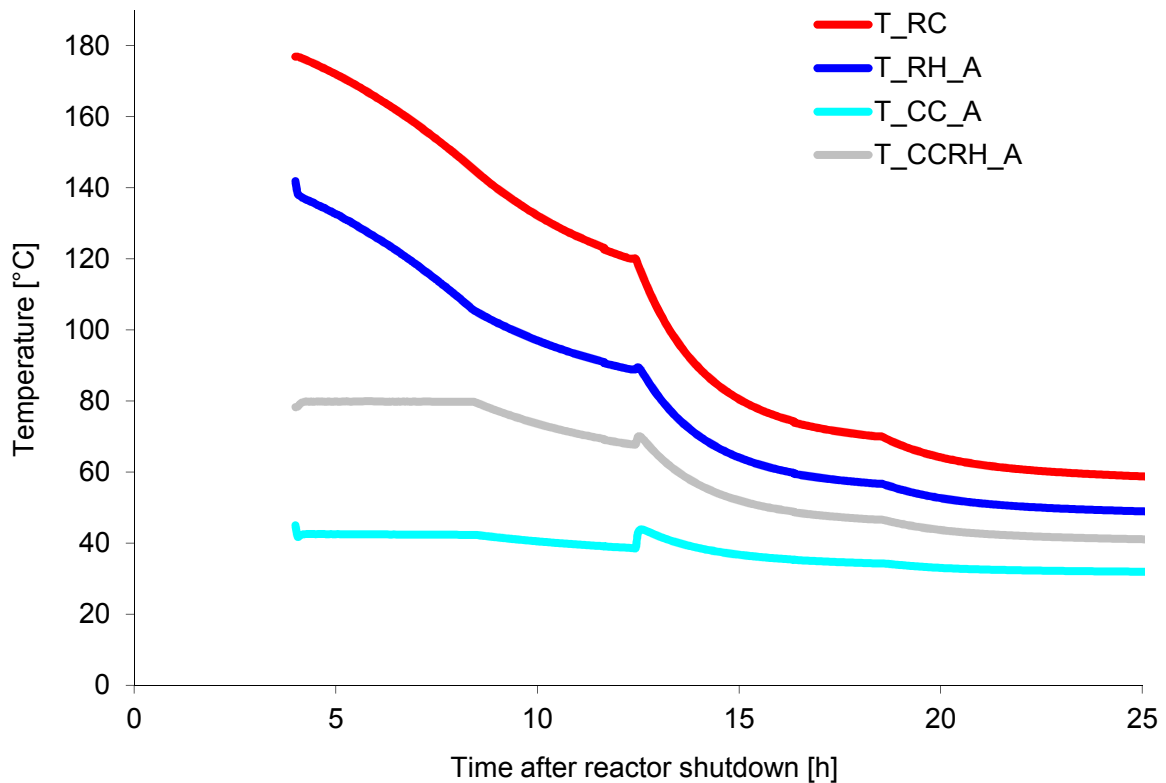


Figure 4.3 – Temperatures in train A generated in the simulation.

When comparing the corresponding temperatures in Figure 4.2 and Figure 4.3 it is clear that there are similarities between the curves. When T_{RC} decreases below 120°C , cooling with the second RH-321 train is initiated and the cooling process is stable for both the measurement data and the simulation, resulting in smoother temperature curves. Before T_{RC} reaches 120°C , the outlet temperatures in the RH-321 heat exchanger (T_{RH_A} and T_{CCRH_A}) are constantly changing according to the measurement data, which is explained by the operators varying the flow through the RH-321 heat exchanger to control the cooling process. In the simulation, this flow is only constrained to prevent T_{CCRH_A} from exceeding 80°C , making the temperature curves much smoother.

Another aspect worth to emphasize is that the difference between T_{RH_A} and T_{CCRH_A} is smaller for the measurement data than for the simulation result. Since a smaller temperature difference corresponds to a higher heat transfer capacity in the heat exchanger, it indicates that the heat transfer capacity is lower in the simulation than in the measurement data. This indication is correct, which will be discussed in Section 4.3-4.4.

To summarize, these comparisons between simulation results and measurement data indicates that the simulated cooldown process gives a good estimation of the real process.

4.2 Comparison with results from the project GREAT

A comparison between results from the GREAT project and the simulation has been performed. A part of the GREAT project was to verify all system criteria, and the results from the verification of the residual heat removal system were used for comparison.

Figure 4.4 shows the reactor coolant temperature over time in the simulation and from the GREAT result. The total cooldown time is slightly longer in the simulation, and there are a couple of reasons for this. The deviation between the curves in the beginning of the process can be explained partly by the flow rate restrictions included in the simulation. The component cooling water has a requirement not to exceed 80°C, which is taken into account in the simulation by reducing the flow of reactor coolant through the RH-321 heat exchanger. To the authors knowledge this flow rate restriction is not included in the GREAT project, allowing for a faster cooldown at high temperatures. Another difference is the UA-value of the CC-711 heat exchanger. In GREAT, the UA-value from the design point in the specification is used (with a correction for change in flow rates). However, in the model presented in this work the UA-value is lower than in the technical design specification (further explained in Section 4.3) which gives an increased cooldown time.

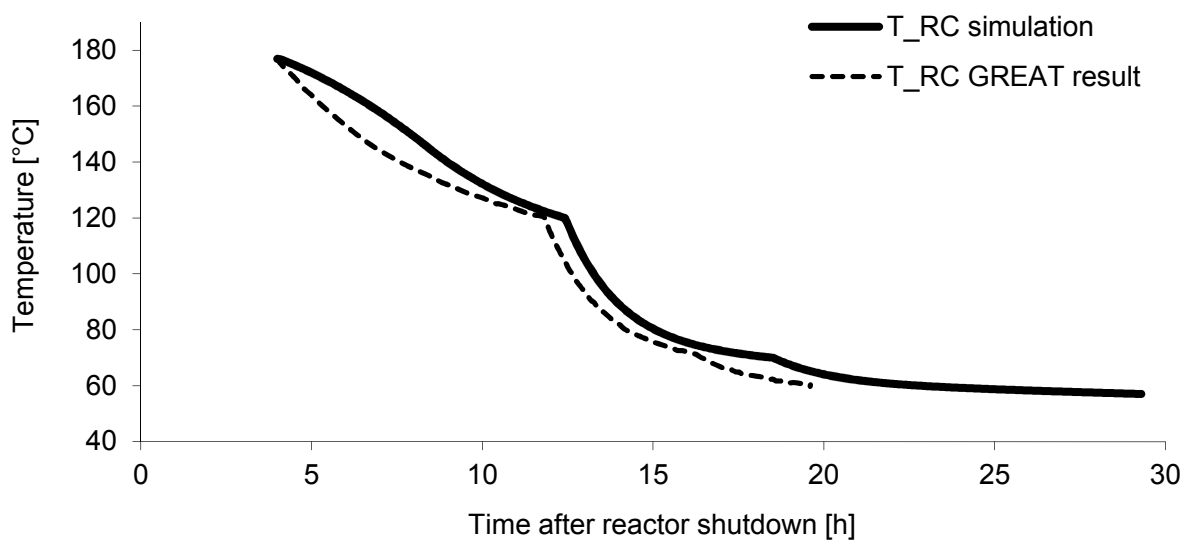


Figure 4.4 – Comparison of simulated reactor coolant temperature (T_{RC}) obtained from the GREAT project and from the simulation.

4.3 Validation of CC-711 heat exchanger sub-model

There are two ways to validate the CC-711 heat exchanger sub-model. Firstly, result from the model can be compared with the heat exchanger specification in the design point, and secondly the results can be compared with performance tests.

The comparison with the specification is presented in Table 4.2. The UA-value calculated by the model is lower than the UA-value stated in the specification. The reason for this is that the dynamic viscosity stated in the specification (0.00036 Pa·s) is not realistic for salt water at the given pressure and temperature [18]. This parameter turned out to have a significant influence on the UA-value. A viscosity of 0.00036 Pa·s in the model generates result almost identical to the value stated in the specification. The model with a correct salt water viscosity is considered valid in this work even though it differs from the specification in the design point.

Table 4.2 - Comparison between heat exchanger specification and used input data in the CC-711 heat exchanger sub-model.

	Heat exchanger specification	CC-711 heat exchanger sub-model
Temperatures tube-side (in/out)	25°C / 49.5°C	25°C / 49.5°C
Temperatures shell-side (in/out)	85°C / 50°C	85°C / 50°C
Flow rate (tube-side / shell-side)	720 kg/s / 504 kg/s	720 kg/s / 504 kg/s
Fouling resistance (tube-side / shell-side)	0.000088 m ² °C/W / 0.000088 m ² °C/W	0.000088 m ² °C/W / 0.000088 m ² °C/W
Viscosity	0.00036 Pa·s	0.000748 Pa·s
UA-value	2466.5 kW/°C	2210.5 kW/°C

By calculating UA-values from measured data and comparing it with capacities calculated by the model, it is possible to further validate the CC-711 heat exchanger sub-model. Data is taken from performance tests carried out in 2007 and 2008 [22, 23].

In the performance tests UA-values was compiled for a number of measurements. These measurements are presented in Appendix G. In Figure 4.5, each measurement is divided into three points on a vertical line. The midpoint represents the time mean (without measurement uncertainties), the point with largest UA-value is given by adding measurement uncertainty to the time mean, and similarly, the smallest UA-value is obtained by subtracting measurement uncertainty to the time mean. The measurement uncertainty is calculated using a two-sided 95% confidence interval, and is based on the estimated accuracy of the instrumentation used in the performance tests [22, 23]. The grey boxes correspond to model calculated UA-values for each measurement. The darker grey areas are the addition due to measurement uncertainties. Two cases are included, no fouling (upper edge) and design fouling (lower edge). It should be noted that design fouling is used in the simulations if nothing else is specifically mentioned.

When analysing the result it can be seen that almost all measurements are within the area between the upper- and the lower edge, even in the cases when measurement uncertainty is accounted for the result is good. To conclude, by using design fouling for the CC-711 heat exchanger in all calculations there is a small risk to overestimate the heat exchangers cooling capability, i.e. the cooling chain's capacity.

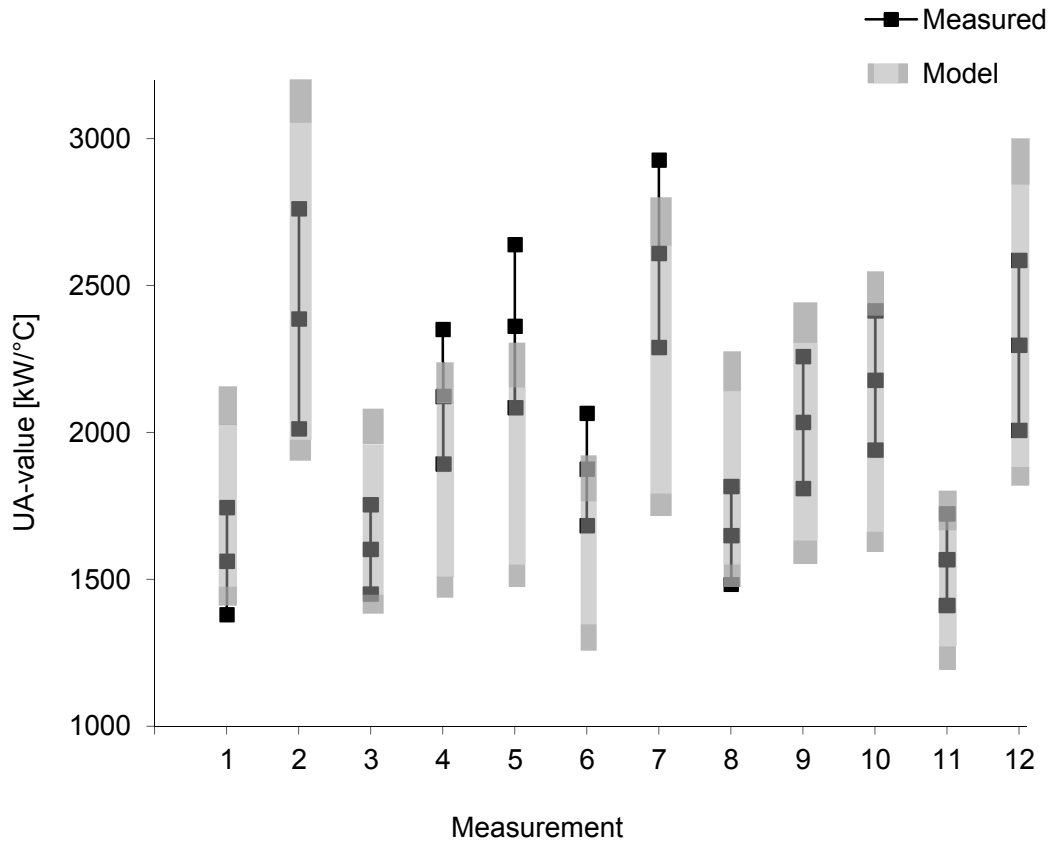


Figure 4.5 – Comparison between measured and calculated UA-values for the component cooling heat exchangers. The grey boxes correspond to UA-values calculated by the model. The darker parts of the grey boxes represent measurement uncertainties.

4.4 Validation of RH-321 heat exchanger sub-model

The validation of the RH-321 heat exchanger sub-model consists of a comparison with the heat exchanger specification only.

The main reason why measured data is not used is because there is a lack of measurement points in the plant. As described in Section 2.2.1, there is a bypass valve in the residual heat removal system that adjust how much of the flow that passes the heat exchanger. The difficulty is that the total flow rate is measured after the downstream mixing point, whereas no instrumentation measures the flow ratio between bypass flow and flow through the heat exchanger, see Figure 4.6. Since the actual flow through the heat exchanger is unknown, estimations of a UA-value based on measured data are uncertain. This problem is discussed further in Section 5.4.

Another aspect is that there are no performance tests with temporary instrumentation available for this heat exchanger, which mean only data from the permanent instrumentation are accessible. The permanent instrumentation is older and more inaccurate, especially the flow meters. Flow measurements are complicated in general, and should preferably be performed in sections of straight piping to avoid eddies. This is not always possible in the plant, which adds to the uncertainty. Also, due to the large temperature range on the tube-side (177°C – 60°C), both flow meters and thermometers are difficult to calibrate for the entire range. In the

performance tests for the CC-711 heat exchangers the instrumentation was better calibrated and more conveniently placed, which resulted in better accuracy.

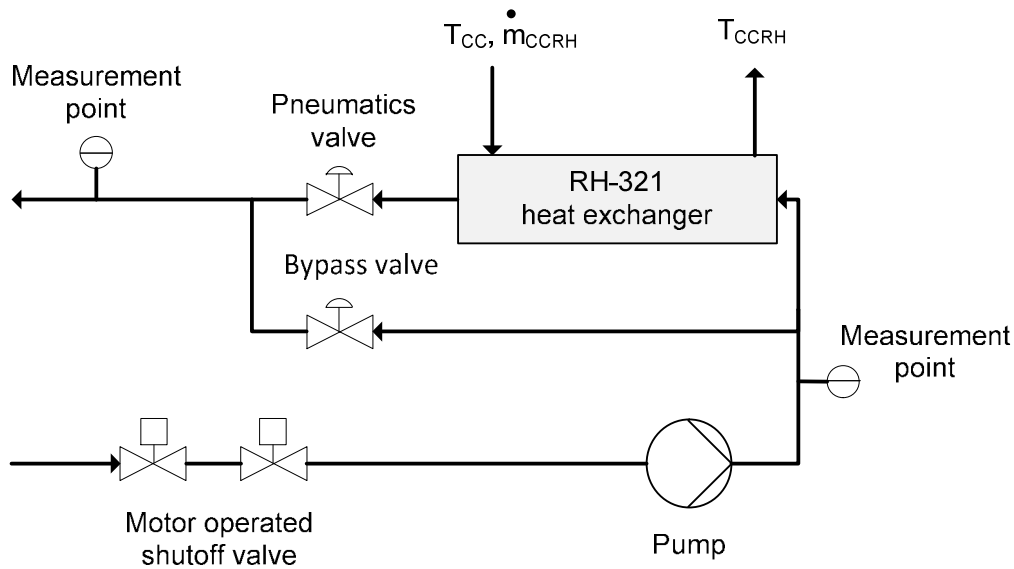


Figure 4.6 - Measurement points around the RH-321 heat exchangers.

The comparison with the heat exchanger specification is presented in Table 4.3. A problem with the RH-321 heat exchanger is that the documentation is deficient, and there is not enough information to satisfactorily calculate the heat transfer coefficient on the shell-side. Since the other terms of the UA-value is comparably easy to calculate, it is reasonable to assume that any error is related to the shell-side heat transfer coefficient. See Appendix C for details regarding Kern's method. The UA-value calculated by the model is slightly higher (622 kW/°C) than the value stated in the specification (590 kW/°C). Since the specification is considered to be correct, the shell-side heat transfer coefficient in the model was adjusted by adding a correction factor of 0.82. By doing this, the UA-value calculated by the model matches the UA-value in the specification. This adjustment is assumed to be valid in the entire cooldown process since the flow rate on the shell-side is kept constant at 252 kg/s in the simulation. The shell-side heat transfer coefficient is therefore almost constant, only affected by variations in temperature. Also, this approach is conservative, which are explained in Section 1.3.

Table 4.3 - Comparison between heat exchanger specification and input data used in the RH-321 heat exchanger sub-model.

	Heat exchanger specification	RH-321 heat exchanger sub-model
Temperatures tube-side (in/out)	59.4°C / 50.6°C	59.4°C / 50.6°C
Temperatures shell-side (in/out)	35°C / 43.3°C	35°C / 43.3°C
Flow rate (tube-side / shell-side)	234.4 kg/s / 252 kg/s	234.4 kg/s / 252 kg/s
Fouling resistance (tube-side / shell-side)	0.00005 m ² °C/W / 0.00009 m ² °C/W	0.00005 m ² °C/W / 0.00009 m ² °C/W
Correction factor for heat transfer coefficient shell-side	n/a	0.82
UA-value	590 kW/°C	590 kW/°C

5 Results

This chapter presents the results of the simulations of Case 1 (normal conditions) and Case 2 (accidental conditions), followed by an investigation of the influence of the sensible heat loads during the cooldown process. Findings regarding the thermal capacity requirements of the heat exchangers are presented, and thereafter a parameter study shows how fouling and plugged tubes affect the cooling chain capacity. Finally, the limiting components in terms of transfer capability in the cooling chain are identified and the impact of flow rates on cooldown time is investigated. The results are based on both simulations and observations made during the construction and validation of the model. Additional simulation results can be found in Appendix H.

5.1 Simulation results

The simulated cooldowns time in Case 1 and 2 are shown in Figure 5.1. In Case 1, a reactor coolant temperature of 60°C is reached 22.8 hours after reactor shutdown. In Case 2, a temperature of 100°C is reached after 24.9 hours. This is much less than 36 hours, which indicates that the requirement of Case 2 is fulfilled. The maximum temperature downstream the CC-711 heat exchanger, T_{CC} , is below the limit of 48.9°C in both cases (maximum 43.8°C and 43.6°C, respectively).

In addition to the obvious difference below a reactor coolant temperature of 120°C, where the second train is placed in operation in Case 1, it can also be seen that the cooldown process in Case 2 is slightly slower before this point. This depends on the fact that there is only one component cooling train available to remove the auxiliary heat loads, where there are two trains in Case 1.

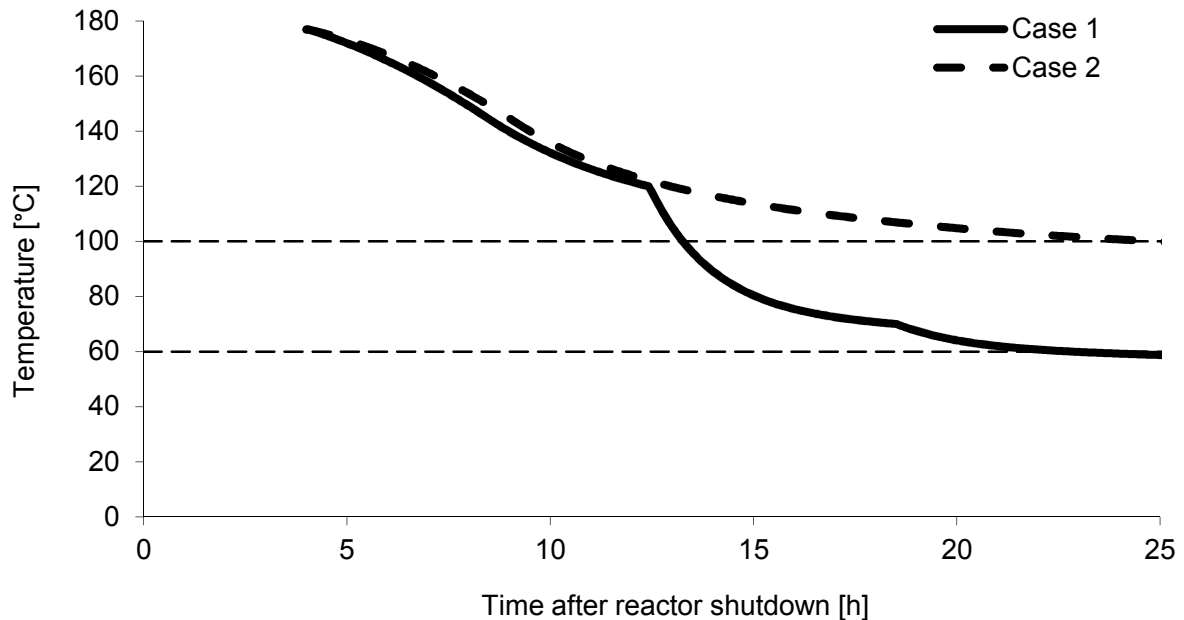


Figure 5.1 – Simulated reactor coolant temperature (T_{RC}) of Case 1 and 2.

The cooldown time depends on many parameters. In Figure 5.2 the cooldown time for Case 1 is shown when the sea water temperature is 16°C compared to 25°C. It also shows the influence of having all sea water pumps (two per train) in operation throughout the whole cooldown process, rather than having only one pump per train when T_{RC} is below 120°C. The mass flow rate with two pumps is 720 kg/s, compared to 420 kg/s with one pump. Operation with two pumps is possible when increased cooling capacity is needed, but should be avoided for longer periods of time due to the risk of pump failure. There is no strict limit on what time span two pumps can be operating simultaneously.

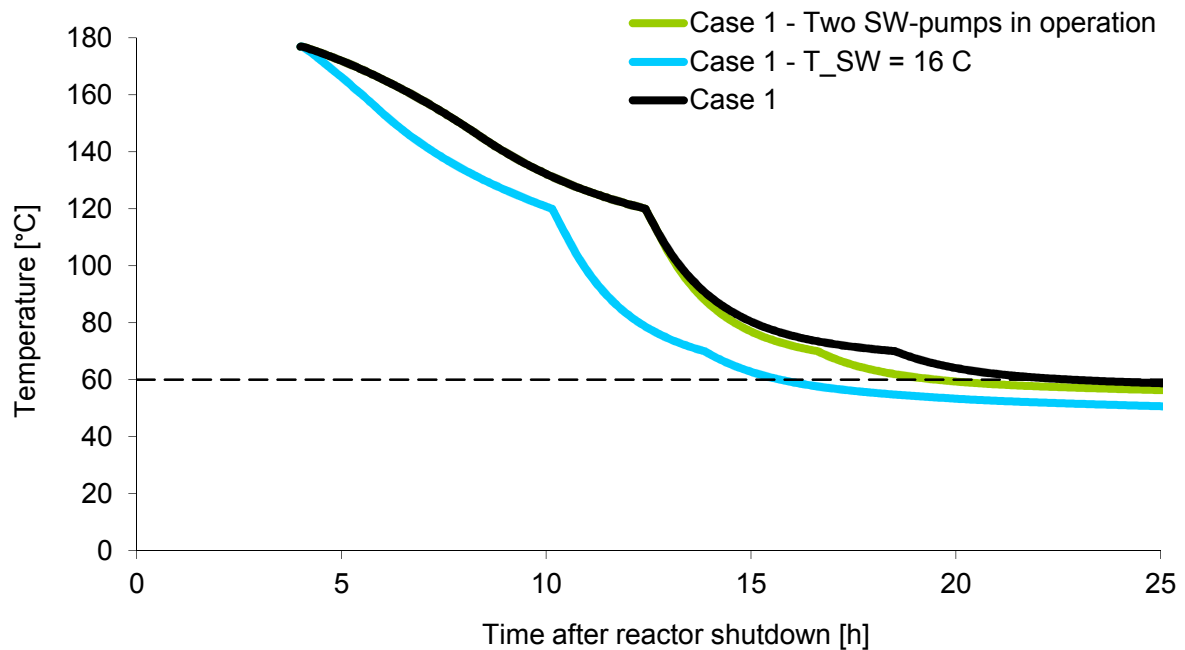


Figure 5.2 - Simulated reactor coolant temperature (T_{RC}) at two different sea water temperatures and varying the number of SW-pumps in operation.

The flow rate in the residual heat removal system is controlled in order to not exceed the maximum absolute temperature gradient ($|dT_{RC}/dt| = 28^{\circ}\text{C}/\text{h}$) and the maximum outlet temperature on the cold side of the RH-321 heat exchanger ($T_{CCRH} = 80^{\circ}\text{C}$). These simulated flow rates are seen in Figure 5.3. The limiting requirement in the beginning is the maximum outlet temperature, which affects train A. For train B, the flow rate is limited by the maximum temperature gradient. The gradient can be seen in Figure 5.4. The curve for Case 2 is shifted slightly to the right, which is explained by the fact that the flow rate is limited by the maximum outlet temperature for a longer time, which in turn depends on the slower cooldown process.

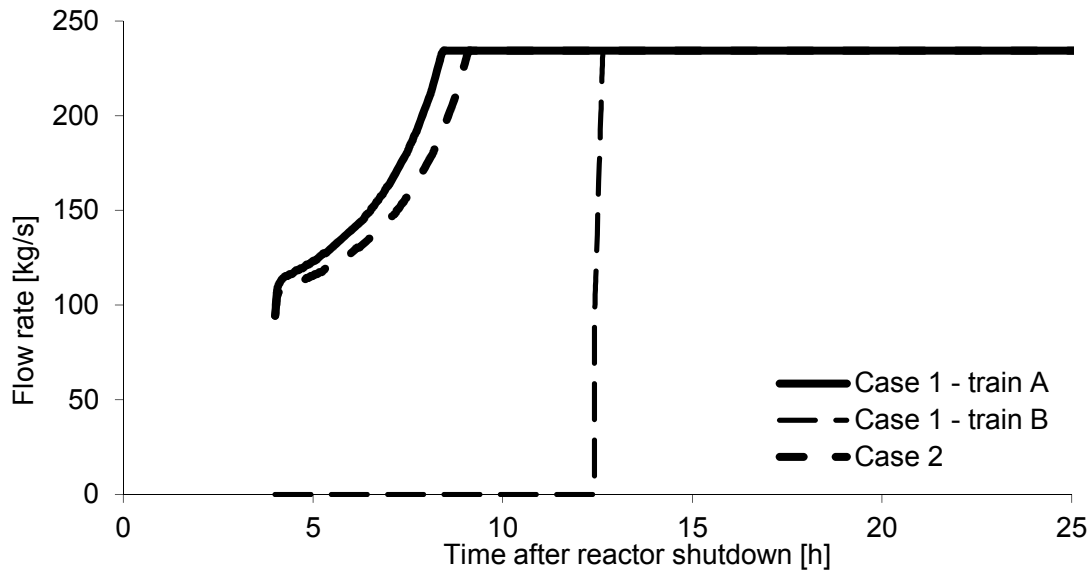


Figure 5.3 - Simulated flow rates in the residual heat removal system of Case 1 and 2.

The absolute temperature gradient in the reactor cooling system, $|dT_{RC}/dt|$, can be seen in Figure 5.4. In Case 1 it is clearly seen that the second train is placed in operation after 12.4 hours, visualized by the largest peak in the curve. It can also be seen that this is the only time the maximum allowable gradient is reached. The peak at 8.4 hours is explained by the fact that the design flow rate in the residual heat removal system is not reached until this point (see Figure 5.3). The gradient then decreases due to lower temperature differences in the system. At 18.5 hours T_{RC} decreases below 70°C and the reactor coolant pump is shut off, which increases the gradient instantaneously. For Case 2, only the leftmost peak is visible. There is no peak in the middle (corresponding to the one at 12.4 hours in Case 1) since the second train is unavailable. Because the reactor coolant pump is not shut off within 25 hours, the rightmost peak is not visible in the graph. This peak will eventually come, but not until 173 hours after reactor shutdown.

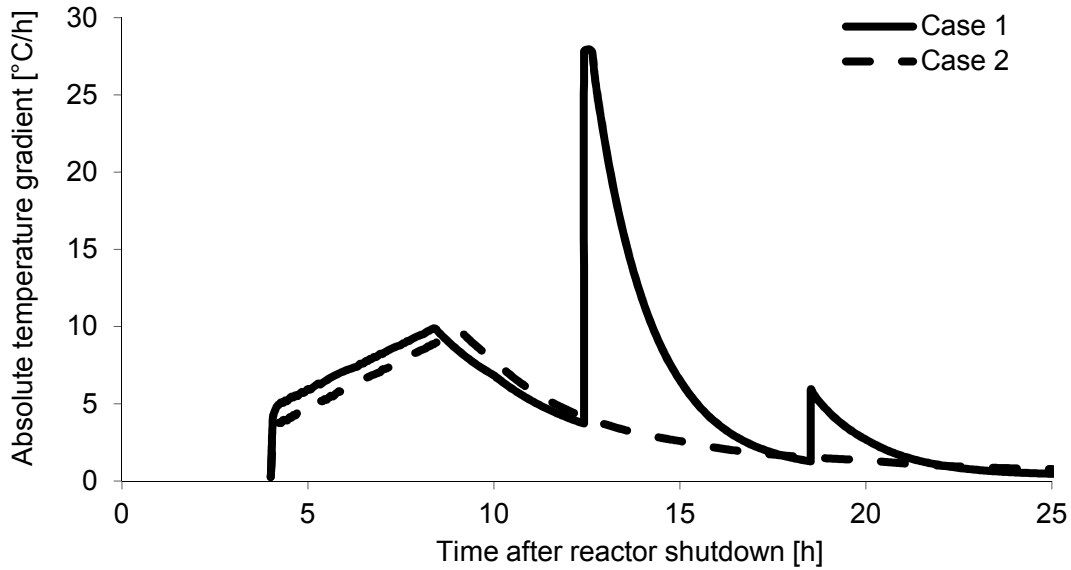


Figure 5.4 – Simulated absolute temperature gradient of the reactor coolant, $|dT_{RC}/dt|$, of Case 1 and Case 2.

Since the requirement on the maximum outlet temperature is closely related to the capacities of the heat exchangers, the requirement on the temperature gradient is the theoretical limit for the cooldown capability. The gradient is far from maximized during large parts of the cooldown process, and it is therefore possible to increase the cooldown capability by investing in equipment with higher capacity. Theoretically, the fastest cooldown is achieved when $|dT_{RC}/dt|$ is equal to 28°C/h during the entire process. Although a cooldown process like this is not possible since it implies infinitely large heat exchangers, the gap between the simulated and theoretical temperature gradient indicates that there is potential for improvement.

5.2 Sensible heat loads during the cooldown process

The impact of the sensible heat load on the cooldown capability during reactor shutdown is not well known, and it is therefore of interest to investigate its importance. The sensible heat load is not included in steady-state analyses. It depends on the reactor coolant temperature gradient and the heat capacity in the reactor cooling system, and is formulated as follows:

$$Q_{sens} = C_{RC} \frac{dT_{RC}}{dt}$$

A comparison between the sensible heat load and the total heat load (Q_{sens} , Q_{RC} and Q_{RCP}) during the cooldown process in Case 1 are presented in Figure 5.5. The sensible heat load curve is proportional to the temperature gradient curve in Figure 5.4, and thus the sensible heat load is highest when the second RH-321 train is placed in operation. It is important to note that after this point, the heat loads seen in the graph are split equally between the two trains. The highest total heat loads on a RH-321 heat exchanger turns out to be between four and eight hours after reactor shutdown, where the maximum heat load is approximately 39.5 MW.

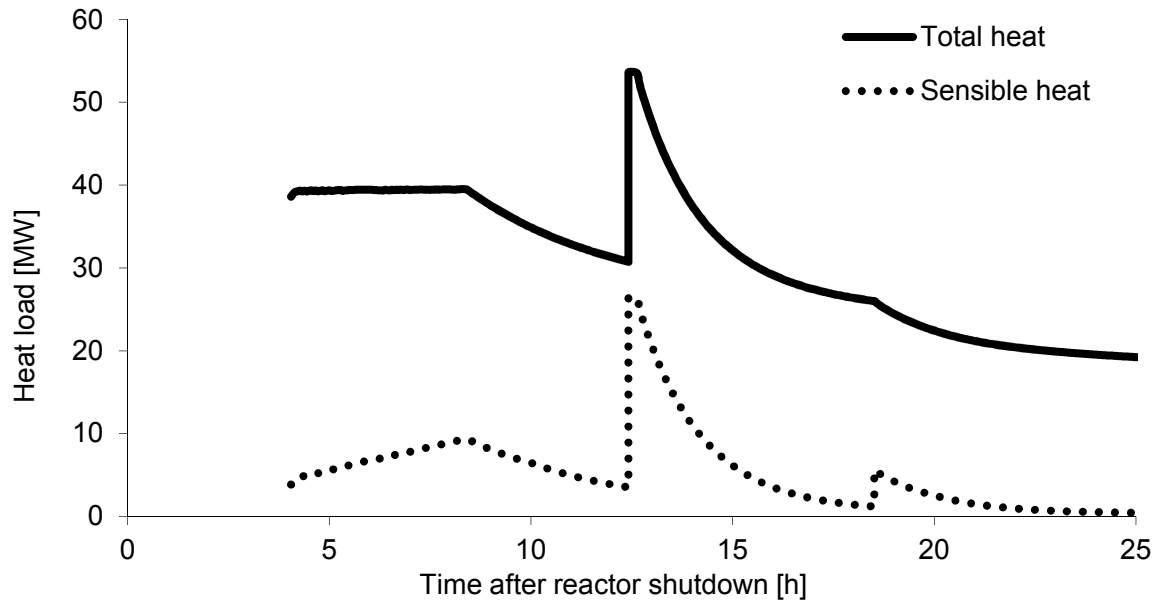


Figure 5.5 – Simulated heat loads during the cooldown process, Case 1.

The sensible heat load varies during the cooldown process, but overall it contributes considerably to the total heat load. In Case 1, the sensible heat (the area under the curve) corresponds to 15.4% of the total heat removed.

To investigate the sensible heat loads further, the assumption regarding the heat capacity of the reactor cooling system is considered. The conservative value used is 3415 MJ/°C. A more realistic value would be approximately 3040 MJ/°C, as described in Appendix B. The effect of heat capacity on the sensible heat load curve during cooldown is seen in Figure 5.6. The new realistic curve is shifted to the left due to a shorter cooldown time. A shorter cooldown time is reasonable since less heat is stored in the reactor cooling system, i.e. less heat to cool. It can also be seen in the graph that the highest peak is slightly lower, which depends on the fact that the maximum gradient is reached more easily. With this heat capacity, the sensible heat corresponds to 14.0% of the total heat.

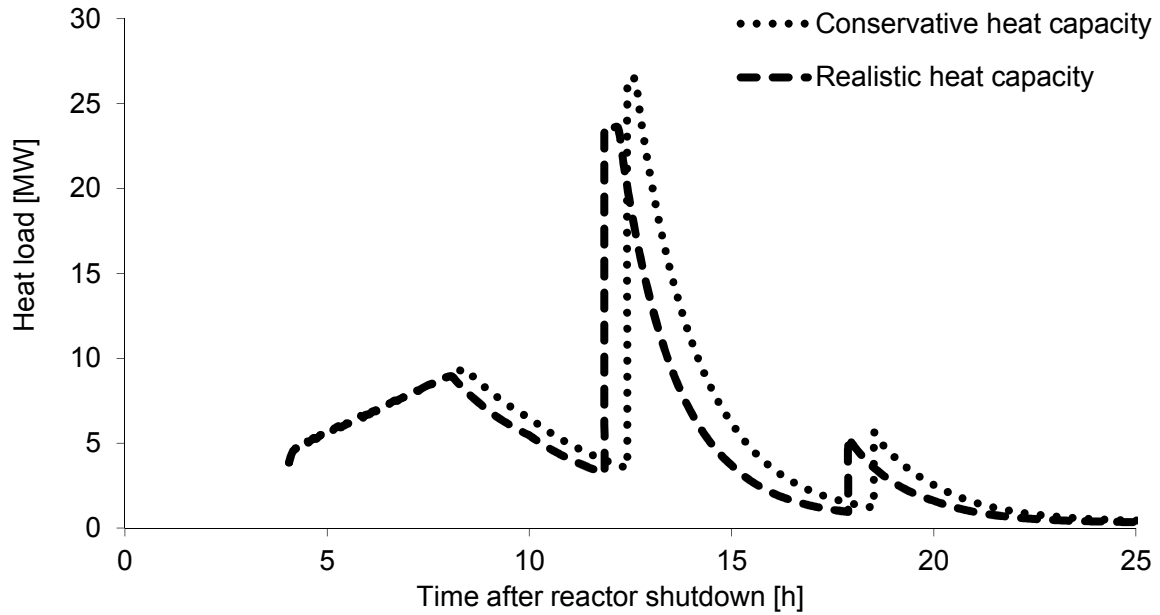


Figure 5.6 - Sensible heat loads for different heat capacities, Case 1.

In Case 2, the contribution from sensible heat is lower, which can be seen in Figure 5.7. Since there is only one train available, the cooldown capability and also the gradient are lower. In Case 2, the sensible heat corresponds to 10.0% of the total heat cooled away.

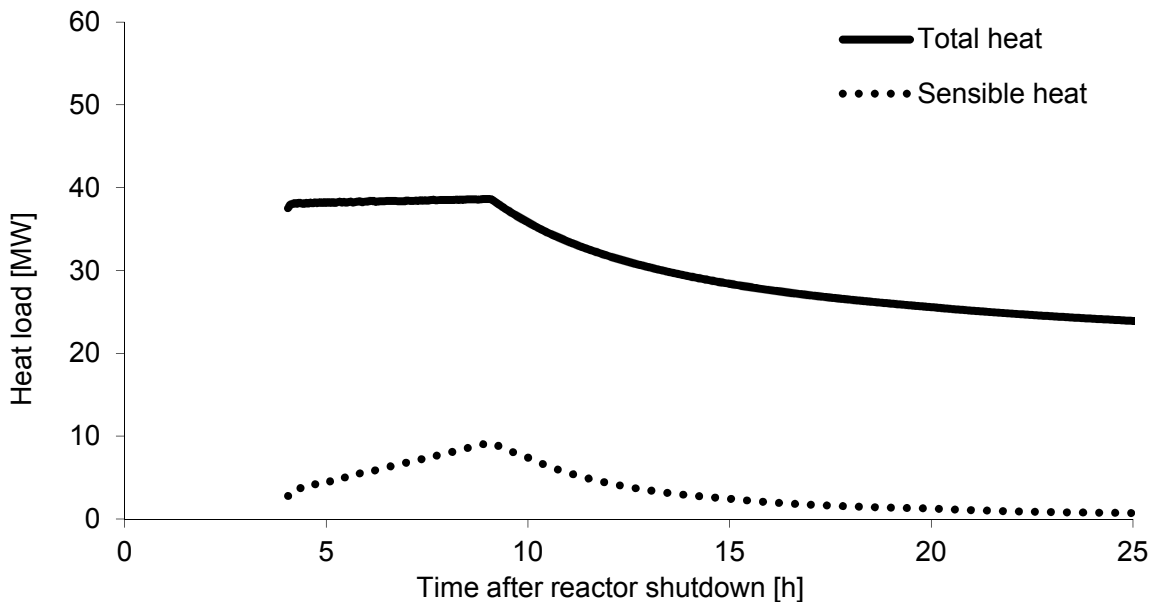


Figure 5.7 – Simulated heat loads during the cooldown process, Case 2.

To summarize, the sensible heat load constitutes a too large share of the total heat load to be neglected when verifying the cooldown capability. This implies that a verification of the cooldown capability should be based on transient calculations. Another observation is that the

heat loads varies a lot during the cooldown process, which affect the heat exchanger capacity verifications. This will be further discussed in Section 5.3.

5.3 Heat exchanger capacity requirements

The heat transfer capacity, UA-value, of a heat exchanger varies with flow rates and temperatures of the passing fluids. In general, higher flow rates and higher temperatures correspond to increased UA-values. This means that the UA-values in the cooling chain’s heat exchangers are not constant. It is therefore necessary to know the variations in UA-value during the cooldown process when specifying a capacity requirement.

This investigation was made by increasing the fouling factor in the heat exchangers to find a simulated cooldown time of exactly 36 hours. Only Case 2 is considered, since no requirement for cooldown time is specified in Case 1. Since the cooldown time is dependent on the capacity of both heat exchangers, finding a specific capacity requirement is complicated. One possible method is to assume a conservative UA-value for one heat exchanger and then to increase the fouling factor of the other heat exchanger in order to find the requirement. This was performed for the two simulations presented in Figure 5.8.

The UA_{CC}-curve was acquired in the case where the fouling factor of the CC-711 heat exchangers was increased to find a cooldown time of 36 hours. Design fouling was used for the RH-321 heat exchanger during this investigation. The UA_{RH}-curve was acquired in the same way, increasing the fouling in the RH-321 heat exchanger while using design fouling in the CC-711 heat exchanger.

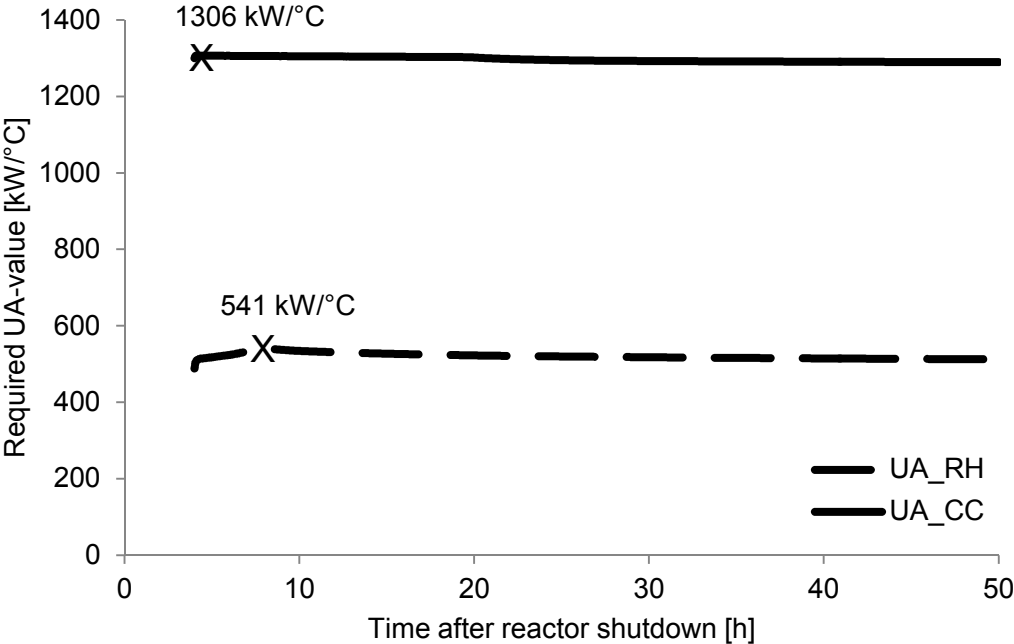


Figure 5.8 - Lowest UA-values required to meet a cooldown time of 36 hours for the RH-321 and CC-711 heat exchangers in Case 2. Note that these curves correspond to two separate simulations.

It can be seen in Figure 5.8 that UA_{CC} is almost constant during the cooldown process. The highest value is found in the beginning and the decrease during the cooldown process is only

marginal. This is due to the constant flow rates and a comparably low temperature decrease. UA_{RH} behaves somewhat differently. It increases in the beginning and has its peak after 7.9 hours, and then slowly decreases. This depends on fact that the flow rate in RH-321 through the RH-321 heat exchanger is increased gradually until this point, see Figure 5.3.

Since these UA-values (1306 kW/°C and 541 kW/°C) are the maximum values during a cooldown process with the longest allowable cooldown time, they could be seen as the heat exchanger capacity requirements. Setting these requirements means that if the measured UA-value for the CC-711 heat exchanger exceeds 1306 kW/°C (including measurement uncertainties) at any given time during the cooldown process, the heat exchanger is good enough for the cooldown time to be shorter than 36 hours. Correspondingly, the measured UA-value of the RH-321 heat exchanger must be at least 541 kW/°C.

There are however some limitations that must be considered. If a measured UA-value is lower than the values stated above, it cannot be said that the heat exchanger requirement is *not* met. The reason that the measured value is lower *could* be that the requirement is not met, but it could also be that the flow rates are lower than the design flow rates used in the simulation. Therefore, if UA-values lower than 1306 kW/°C or 541 kW/°C are measured, it must be more thoroughly analysed whether the heat exchanger meet its requirements or not.

It should also be mentioned that flow rates higher than design is possible, although uncommon. If this is the case the values above is not valid, since a higher flow rate will give a higher UA-value which cannot be compared to 1306 kW/°C or 541 kW/°C without consideration.

One issue that should be focused a bit more upon is that the highest UA-value for the RH-321 heat exchanger is not in the beginning of the process. Intuitively, one would think that the highest temperatures and flow rates, and therefore also the highest UA-values, are found just after the cooling chain is placed in operation, i.e. at four hours after reactor shutdown. However, since the simulation is transient it is included that the flow rate varies in the beginning, which has the consequence that the highest UA-value is reached later in the process. This means that transient calculations are necessary when finding the heat transfer capacity requirement for the RH-321 heat exchanger.

These requirements are based on the assumptions that only one of the heat exchangers has a decreased UA-value (i.e. fouling factor higher than design). It could however be possible that both heat exchangers will have decreased UA-values simultaneously, and it is therefore desirable to find all possible combinations of UA-values that give a cooldown time of 36 hours. This is performed and presented in Figure 5.9. Note that the maximum UA-value of each heat exchanger during the cooldown is chosen when making the curve. If a measured combination of UA-values is located to the right of the curve, the cooldown time will be shorter than 36 hours and the system requirement is fulfilled. Limitations do however apply to the investigation in Figure 5.9 as well. Measured combinations to the left of the curve does not necessarily mean that a cooldown time of maximum 36 hours will be exceeded. More analysis of the measured flow rates and temperatures is needed before any conclusions can be drawn.

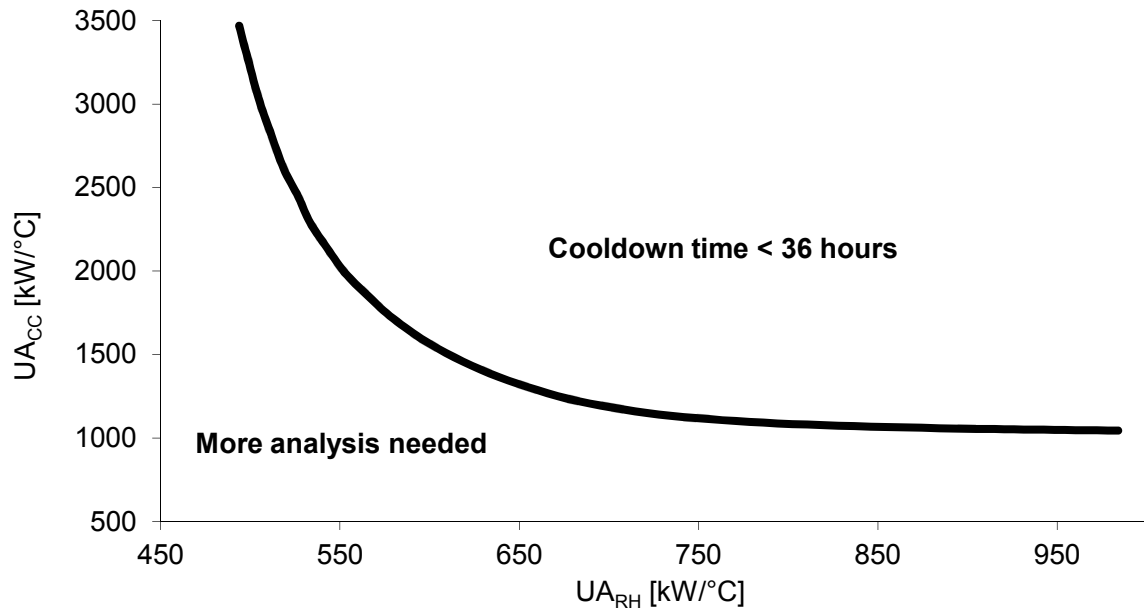


Figure 5.9 – Combinations of UA-values for the heat exchangers resulting in a cooldown time of 36 hours in Case 2.

5.4 UA-value measurements for the RH-321 heat exchanger

As mentioned in Section 4.4, estimations of UA-values for the RH-321 heat exchangers from measured data are uncertain due to the lack of measurement points. The lack of measurement points has the consequence that only the combined flow through the bypass and the heat exchanger is known (see Figure 4.6). A measured UA-value based on the assumption that the full flow passes through the heat exchanger is unreliable and should be avoided if possible. Despite this, measured data can be used to indicate the heat exchanger performance to some extent. By studying the measured temperature curves during the cooldown process 2011 in Figure 5.10, it can be seen that at any given time there is a relation between the UA-value and the difference between the outlet temperatures on each side (T_{RH} and T_{CCRH}). The bigger the temperature difference is, the lower the UA-value. Similar behaviour was found for measured data during cooldown processes 2008 to 2010. This depends on the fact that when the flow through a heat exchanger is increased, the difference between the outlet temperatures is decreased.

Therefore, when estimating the UA-value of the RH-321 heat exchanger from measured data, the data should be taken in intervals where T_{RH} and T_{CCRH} are close together. This way the real flow rate is better estimated, and the UA-value will be more accurate. This is the most favourable option for verification of the heat exchanger performance with existing measurement points. It should however be remembered that the uncertainties discussed in Section 4.4 are large, and results should be considered carefully.

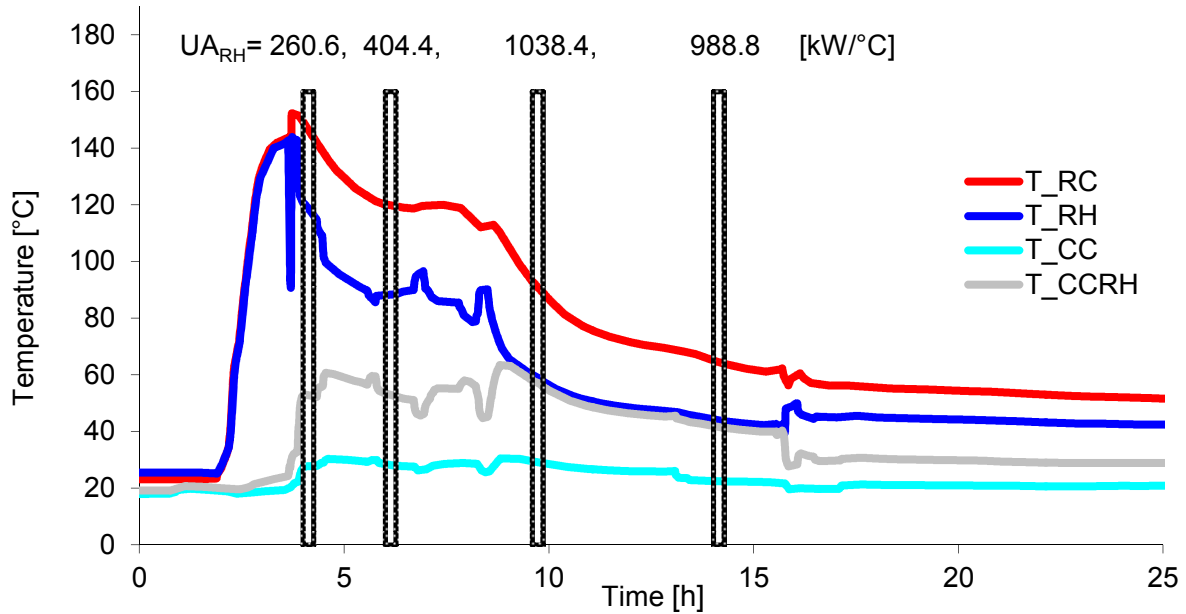


Figure 5.10 - Measured inlet and outlet temperatures of the RH-321 heat exchanger in train A during the cooldown process in 2011.

5.5 Influence of plugged tubes in the heat exchangers

Tube plugging occurs due to structural degradation of heat exchanger tubes, especially common in tubes exposed to raw water. A degraded tube may lead to leakage which affects the heat transfer capacity of the heat exchanger. By plugging the degraded tube, fluid leakage can be avoided. Since the heat transfer capacity of the heat exchanger is reduced with the number of plugged tubes, it is of interest to find the maximum number of plugged tubes in the heat exchangers while the cooldown time requirement is fulfilled. The analysis was made only for Case 2 since no corresponding requirement exists for Case 1.

An important aspect is that flow regime in the heat exchangers is altered when plugging tubes, and that the method used is not sufficient for large numbers of plugged tubes. The investigation was still carried out, but the results for plugging degrees (plugged tubes in relation to total number of tubes) exceeding 10% should be considered with caution.

Sensitivity analysis was conducted for both the CC-711 and RH-321 heat exchanger. It is assumed that no tubes are plugged in the CC-711 heat exchanger when investigating the RH-321 heat exchanger and vice versa. When simulating, only one parameter (number of plugged tubes) is changed at a time.

Figure 5.11 presents the cooldown time as a function of plugging degree for both the CC-711 heat exchanger and the RH-321 heat exchanger. The requirement of maximum 36 hours cooldown time is indicated in the figure with a dashed line. By comparing the two curves it can be concluded that the cooling chain is more sensitive to tube plugging in the RH-321 heat exchanger than in the CC-711 heat exchanger. The underlying reason for this is partly related to the difference in configuration (number of passes) between the heat exchangers. Since the RH-321 heat exchanger has two tube passes, plugging of tubes provides a larger percental decrease of heat transfer area than in the CC-711 heat exchanger where there is only one tube pass.

Another factor to consider is that the total number of tubes is much greater in the CC-711 heat exchanger (2442 tubes) than in the RH-321 heat exchanger (415 tubes). This means that it is possible to plug 1191 tubes in the CC-711 heat exchanger without exceeding 36 hours, while the corresponding number for the RH-321 heat exchanger is 79. Together with the fact that the tubes in the CC-711 heat exchanger are made of titanium, which makes the need for plugging less likely, it is obvious that plugged tubes in the RH-321 heat exchanger are more critical. It must however be remembered that the validity of the calculation method is uncertain at high plugging degrees. Currently there are not any plugged tubes in either heat exchanger, and therefore tube plugging should not be a concern with respect to the cooldown time requirement.

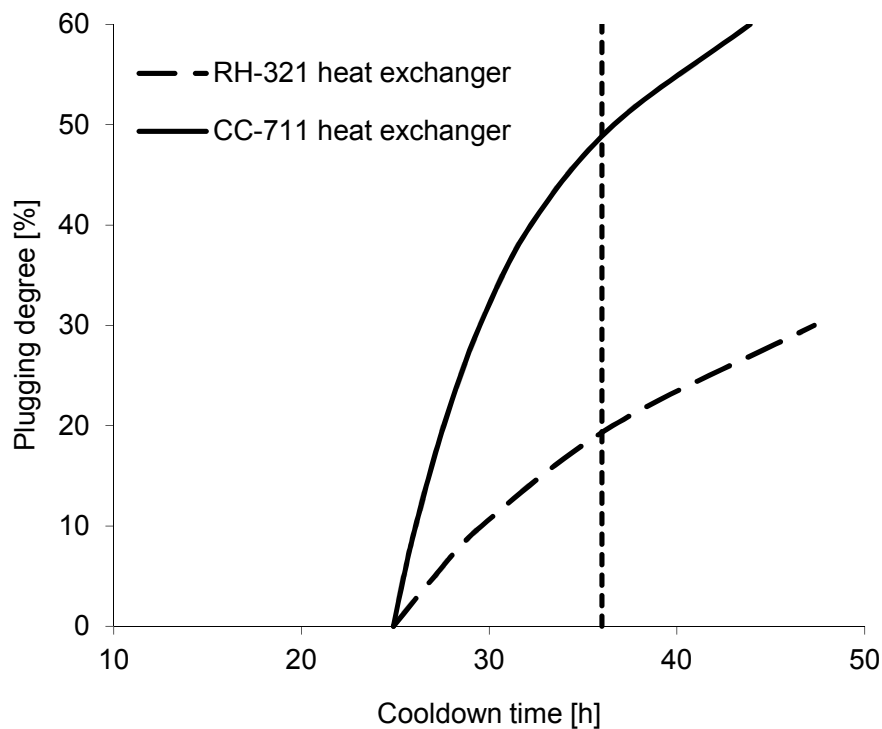


Figure 5.11 - Change in cooldown time due to plugged tubes in the CC-711 and RH-321 heat exchanger for Case 2. The vertical dashed line indicates the cooldown time requirement of 36 hours.

5.6 Influence of fouling in the heat exchangers

Problem with additional resistance on heat transfer areas occurs due to deposit of biological and chemical material, commonly referred to as fouling. Fouling decreases the heat transfer capacity in heat exchangers, and is strongly dependent on the tube wall material and the fluid properties as well as flow velocities. To ensure that the heat transfer capacity needed in a process is met, standard values for fouling is used when designing a heat exchanger. These values are called the design fouling of the heat exchanger. It is of interest to see how the process is affected by values greater than design fouling in order to investigate when the cooldown time requirement is violated. The analysis was performed for both Case 1 and Case 2, where the latter was studied in more detail due to this requirement.

In simulations it is assumed that the fouling factors on the tube- and shell-side are changed proportionally. In the analysis considering the RH-321 heat exchangers, design fouling is used for the CC-711 heat exchangers and vice versa. Figure 5.12 shows the simulation results for Case 2 together with a vertical dashed line indicating the requirement on cooldown time. By studying the figure, it can be concluded that the cooldown time is satisfied even at high level of fouling for both the RH-321 heat exchangers and the CC-711 heat exchangers. It can also be seen that the RH-321 heat exchangers is more sensitive to fouling than the CC-711 heat exchangers. The maximum allowable fouling for the RH-321 heat exchangers is 163% of the design fouling and the corresponding values for the CC-711 heat exchangers is 272.5%. When evaluating these numbers, it is important to note that the CC-711 heat exchangers are exposed to sea water on the tube-side which generally contributes to high level of fouling. To diminish the effect of this fouling a purification system is used for tube cleaning in the CC-711 heat exchangers. It should also be mentioned that the RH-321 heat exchangers is not exposed to fluids that contributes much to fouling. Often, these heat exchangers are considered to be “clean” which means that the real level of fouling is almost negligible.

Since high level of fouling in general only exist on the tube-side of the CC-711 heat exchangers, a modified simulation was performed. Design fouling was assumed for all heat transfer surfaces in the cooling chain except for the tube-side in the CC-711 heat exchanger. Under these conditions, the maximum allowable tube-side fouling without exceeding the cooldown time requirement was 432% of the design fouling.

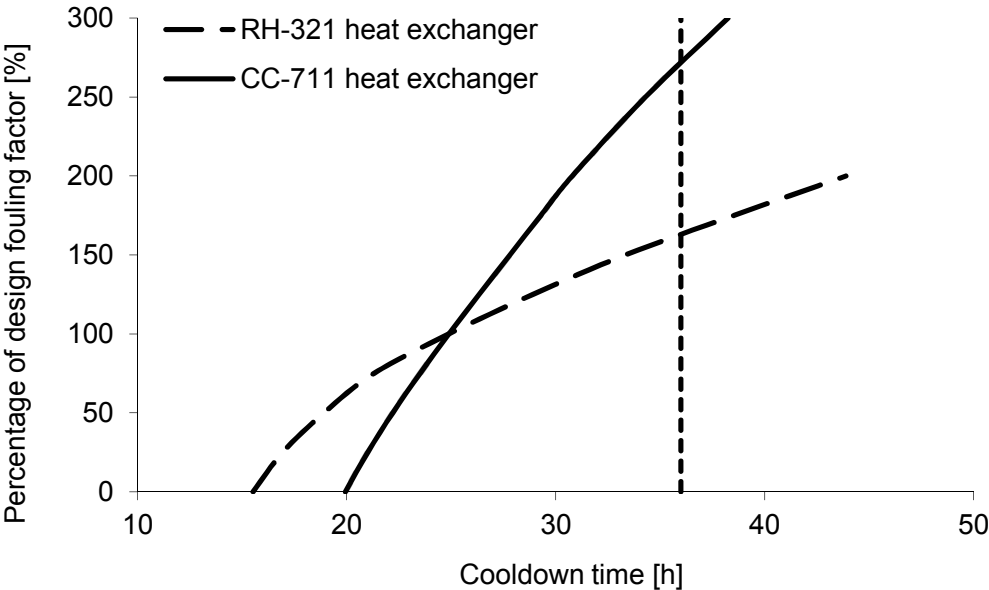


Figure 5.12 - Change in cooldown time due to fouling in the heat exchangers for Case 2. The vertical dashed line indicates the cooldown time requirement of 36 hours.

The simulation result for Case 1 is given in Figure 5.13. The figure shows the impact fouling has on the cooling capacity in terms of cooling capability when two trains are.

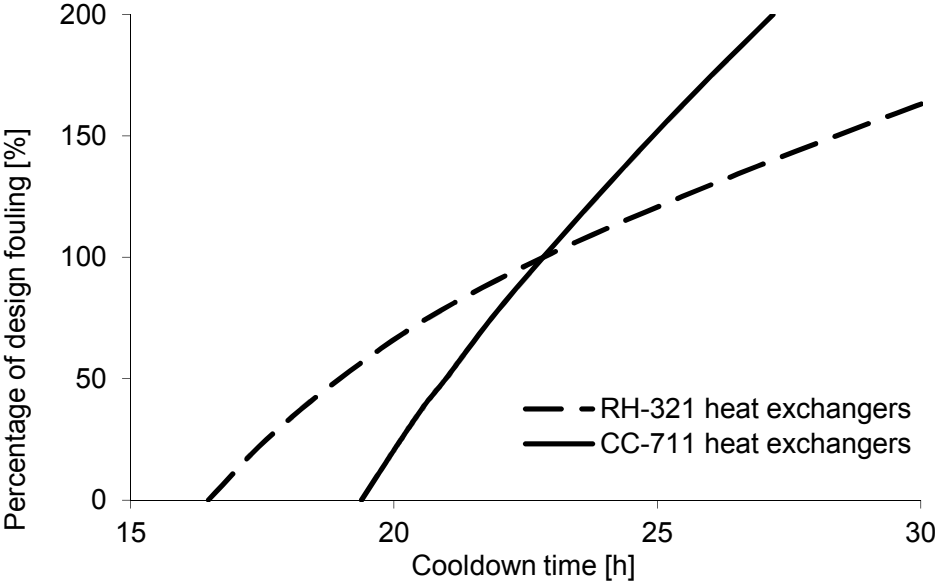


Figure 5.13 – Change in cooldown time due to fouling in the heat exchangers for Case 1.

5.7 Limiting components

In order to gain understanding of the thermal limitations of the cooling chain, it is of interest to investigate which heat exchangers in the cooling chain are limiting the cooldown capability. To evaluate this, a sensitivity analysis for Case 1 has been conducted.

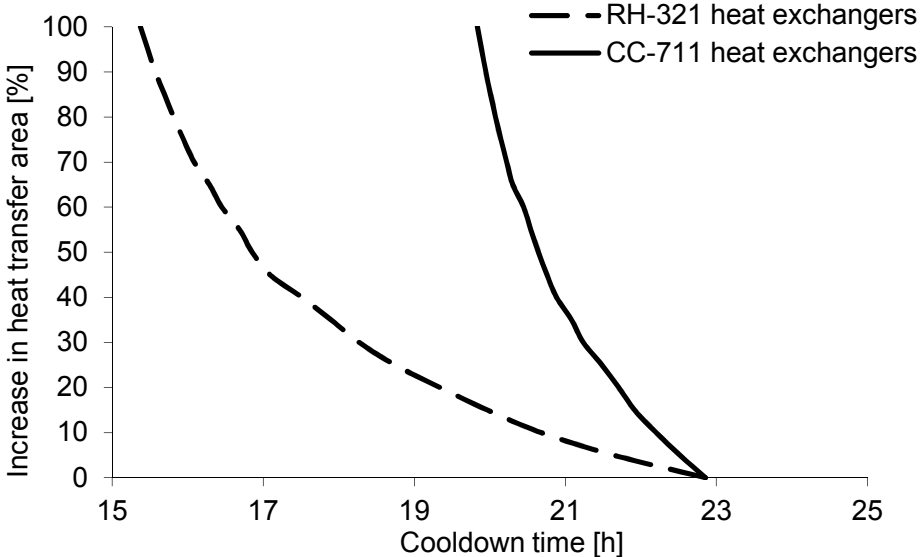


Figure 5.14 – Cooldown time as function of heat transfer area for Case 1.

The limiting heat exchanger can be found by investigating the relationship between heat transfer area and cooldown time. In the case where the RH-321 heat exchangers are investigated, the heat transfer area of the CC-711 heat exchangers is constant, and vice versa. The simulation results are given in Figure 5.14. The cooldown time decreases more rapidly for the RH-321 heat exchangers than for the CC-711 heat exchangers, which means that the RH-321 heat exchangers limit the cooldown capability.

5.8 The impact of flow rates on cooldown time

A sensitivity analysis of flow rates impact on cooldown time for Case 1 is illustrated in Figure 5.15. This investigation provides improved understanding of how the flow rates affect the cooldown time when the transient heat loads are taken into account. The cooling chain’s capability is at small variations more sensitive to flow rate changes the closer to the heat source the flow is. This means that if the flow rate in the residual heat removal system is decreased, the increase in cooldown time is greater than if the sea water flow rate is decreased. However, at a flow rate decrease of more than 40%, the flow rate in the component cooling system is more sensitive. Thus, it is more important to monitor the flow rates in the residual heat removal and the component cooling systems than in the salt water system to ensure an efficient cooldown process. In addition, it is clear that increased flow rates do not affect the cooldown time to any great extent. Improvements that increase the flow rate will therefore have limiting benefit in terms of cooldown capability. It must however be remembered that this is only valid given that there is a requirement on the maximum temperature in CC-711. Since this requirement limits the RH-321 flow rate in the beginning of the process, increasing the flow rate capacity in RH-321 will give a lower contribution than if the flow rate was not limited.

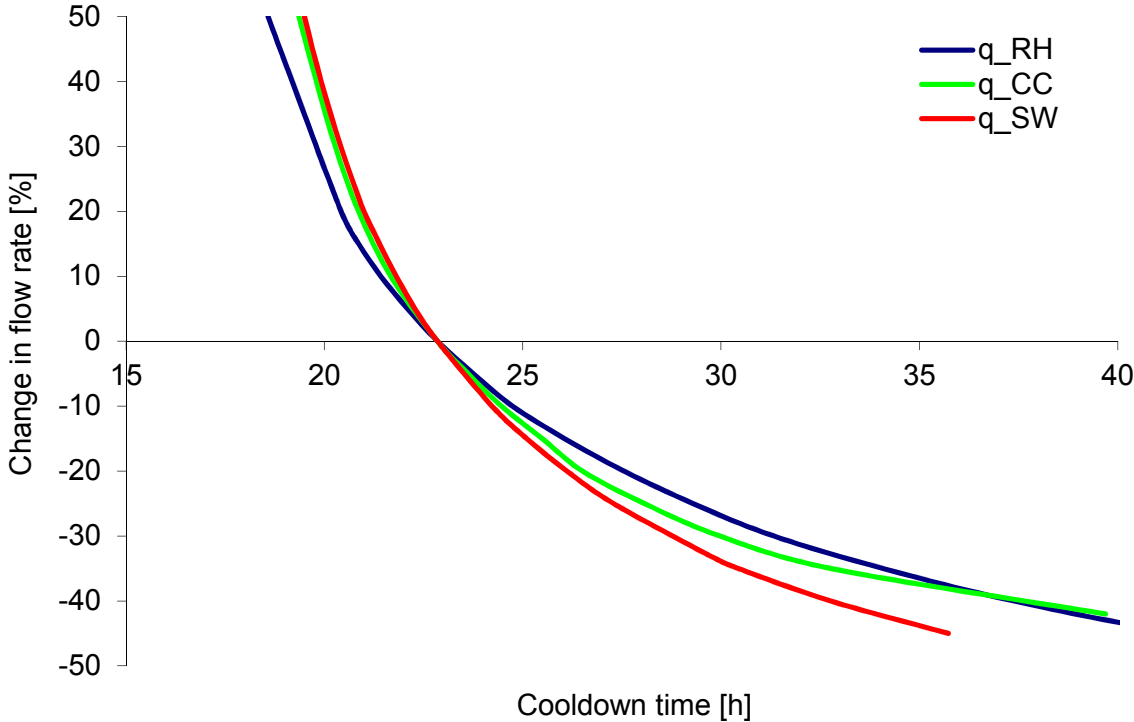


Figure 5.15 – Change in cooldown time due to changed flow rates for Case 1.

6 Conclusion

This thesis investigates the transient heat loads in the cooling chain for decay heat during the reactor shutdown process. A transient computational model of the cooling chain was constructed and the investigation was based on simulations performed with this model. The model was successfully validated by comparing with measurements in the plant and with results from a comparable project.

The results show that it is crucial to consider the transient behaviour of the cooling chain when simulating the cooldown process and verifying the cooldown capability of the residual heat removal system, as it is required to account for the sensible heat stored in water and structural material. The sensible heat corresponds to 10 - 15% (depending on operational mode) of the total heat cooled away. In addition, the sensible heat load is proportional to the reactor coolant temperature gradient and therefore varies in an unpredictable manner during the process.

The required heat transfer capacities of the CC-711 and RH-321 heat exchangers are determined to be 1306 kW/°C and 541 kW/°C, respectively. If the measured heat transfer capacities are larger than these values, the requirement of a cooldown time of maximum 36 hours during accidental conditions (only one train available) is fulfilled.

Fouling values up to 163% and 273% of the design fouling (for the RH-321 and the CC-711 heat exchangers, respectively) are allowed for a cooldown time of 36 hours. The capacities of the heat exchangers are sufficient without any concerns for fouling. However, fouling is complicated to measure and poorly documented at Ringhals 3, and it is recommended to conduct a measurement campaign on fouling that could be related to the simulation results. The margin for plugging tubes is large, and should not be a concern to the cooldown time requirement.

The RH-321 heat exchanger is the limiting component to the cooldown time. Upgrading this heat exchanger will have the largest increase of the cooldown capability, whereas improvements to increase the flow rates will have limited effect on the cooldown capability.

Finally, there are some recommendations for further work. Firstly, investigating how the heat transfer capacities stated above change with flow rates will lead to a more comprehensive picture of how to verify the performance of the heat exchangers. This is necessary to be able to set general requirements. Secondly, the real fouling values of the heat exchangers should be documented on a regular basis. Improved documentation will increase the knowledge of the heat exchanger performance and put the maximum allowable fouling values suggested above in relation.

7 References

- [1] **Vattenfall AB, 2012.** *Om Ringhals*. [Online] February, 2012
<http://www.vattenfall.se/sv/om-ringhals.htm>
- [2] **Westinghouse, 2006.** Ringhals 3 – GREAT, Residual Heat Removal System – Cooldown capability, 2006: Ringhals AB, 2006. In-house. Darwin ID* : 1907420.
- [3] **Nordlund, Anders. 2011.** *Introduction to Nuclear Reactors*.
- [4] **KSU, 2011.** *Reaktorkylsystemet RC-313: Kärnkraftsäkerhet och Utbildning AB, 2011*. In-house: R34-ARO-313.
- [5] **KSU, 2005.** *Kylsystem reaktor: Kärnkraftsäkerhet och Utbildning, 2005*. In-house: R34-002.
- [6] **KSU, 2007.** *Komponentkylvattensystem CC-711: Kärnkraftsäkerhet och Utbildning, 2007*. In-house: R34-RSK-711-50.
- [7] **KSU, 2007.** RSK SW-715: *Kärnkraftsäkerhet och Utbildning, 2007*. In-house: R34-RSK-715-50.
- [8] **Westinghouse, 2006.** *Ringhals GREAT – Decay heat models, 2006*: Ringhals AB, 2006. In-house: WB-GREAT-WR-5.9. Darwin ID* : 1906684.
- [9] **Ringhals AB, 2011.** *R3 SAR Systemdel Kapitel 9.2 - Water systems, 2011*: Ringhals AB, 2006. In-house. Darwin ID* :1602715.
- [10] **Westinghouse, 2010.** *Ringhals 3 GREAT – Plant input data document, 2010*: Ringhals AB, 2010. In-house: WB-GREAT-WR-11. Darwin ID* :1906684.
- [11] **Ringhals AB, 2011.** *R3 Avställning från varm beredskap till kall avställning, 2011*: Ringhals AB, 2011. In-house. Darwin ID* :1882708.
- [12] **Bergman, T. Et al, 2007.** *Fundamentals of Heat and Mass Transfer*. John Wiley Sons, USA, 6th edition.
- [13] **Westinghouse, 2006.** *Ringhals 3 GREAT – Component Cooling Water System, 2006*: Ringhals AB, 2006. In-house: WB-GREAT-WR-8.7. Darwin ID* :1907425.
- [14] **Ringhals AB, 2008.** *Teknisk specifikation Mek – Värmeväxlarspecifikation 30711 CCAHCC-01/02, 2008*: Ringhals AB, 2008. In-house. Darwin ID* :1978023.
- [15] **Ringhals AB, 1973.** *RH-specifikation, 1973*: Ringhals AB, 1973. In-house. Darwin ID* :1841818.
- [16] **Ringhals AB, 1973.** *Värmeväxlarritning, 1973*: Ringhals AB, 1973. In-house. Darwin ID* :7002649.
- [17] **Ringhals AB, 1973.** *Heat exchanger performance – document, 1973*. In-house: 3C302.1.

- [18] **Mostafa H. Sharqawy, John H. Lienhard V, and Syed M. Zubair, 2010.** "Thermophysical properties of seawater: A review of existing correlations and data," *Desalination and Water Treatment*, Vol. 16, pp.354-380, April 2010. [Online] March 2012, <http://web.mit.edu/seawater/>.
- [19] **MatlabCentral, 2012.** X-steam, Thermodynamic properties of Water and Steam, 2007. Based on: *The International Association for the Properties of Water and Steam, 2007. Revised Release on the IAPWS Industrial Formulation 1997 for the Thermodynamic Properties of Water and Steam.* [Online] March 2012. <http://www.mathworks.com/matlabcentral/fileexchange/9817>
- [20] **Sinnott R.K., 2005.** *Chemical Engineering Design – Volume 6.* Butterworth-Heinemann Ltd, UK, 4th edition.
- [21] **Ringhals AB, 2011.** *R3 Avställning från varm beredskap till kall avställning, 2011.* In-house. Darwin ID*:1882708.
- [22] **Ringhals AB, 2007.** *Provrappport, Systemprov Nivå II, Kontroll av CCAHCC-01/02 – direkt efter installation – i DT7, 2007.* In-house. Darwin ID*:1954407.
- [23] **Ringhals AB, 2009.** *Provrappport, Prestandaprov nivå II, Kontroll av CCAHCC-01/02 – Under RA08 – i DT5 och DT7, 2009.* In-house. Darwin ID*:1981846.
- [24] **Ringhals AB, 2007.** *Westinghouse Answers to RAB Review notes WB-GREAT-8.3 – rev1, 2007.* In-house. Darwin ID*:1942379.

*Darwin is a document handling system used at Ringhals. Each document is named with a number so called Darwin ID.

Appendix A – Decay heat load

The decay heat table used as input data to all simulations is given in Table A.1. The given values consider fission products, actinides and activated structural materials.

Table A.1 – Decay heat load for a 12 month fuel cycle [7].

Time after shutdown	Decay heat load, 12 month fuel cycle [MW]
4 hours	30.39696
10 hours	24.00871
15 hours	21.54229
20 hours	19.89801
30 hours	17.69823
40 hours	16.20949
50 hours	15.08738
60 hours	14.19858
62 hours	14.03193
70 hours	13.45421
85 hours	12.53208
95 hours	12.00991
110 hours	11.43331
120 hours	10.95224
130 hours	10.59894
135 hours	10.4334
150 hours	9.980113
8 days	8.969103
10 days	8.128076
15 days	6.809487

Appendix B – Heat capacity RC-313

Sensible heat is represented by the heat capacity. In Table B.1-B.4 the masses that store energy in the reactor cooling system are given. These masses characterize a 3 loops Westinghouse nuclear power plant, which is a similar plant to Ringhals 3 [24].

Table B.1 – Metal masses.

Metal masses	[kg]
Pressurizer	85000
Reactor vessel	389900
3 hot leg piping	19740
3 cold leg piping	23820
3 RCPs	122340
3 steam generators	1052970
$m_{\text{Tot,metal}}$	1693770

Table B.2 – Reactor cooling water masses.

Primary RC water mass	
Volume in RC system at T_{hot}	63.26 [m ³]
Volume in RC system at T_{cold}	106.7 [m ³]
Volume in RC system at T_{average}	88.13 [m ³]
Volume pressurizer	40.78 [m ³]
$m_{\text{Tot,RCwater}}$	298.87 [kg]

Table B.3 – Water mass in the steam generators.

Secondary water mass in steam generators	[kg]
Water mass	225833
$m_{\text{Tot,steamwater}}$	225830.3

Table B.4 – Physical properties.

Physical properties	
Specific heat capacity metal, $c_{p,metal}$	0.523 [kJ/kg K]
Specific heat capacity water, $c_{p,water}$	4.375 [kJ/kg K]
Density water at 30.3 bar and 176.7°C, ρ_{water}	891.971 [kg/m ³]

The actual heat capacity for a 3 loops Westinghouse nuclear plant is calculated as:

$$C_{RC} = m_{Tot,metal} c_{p,metal} + m_{Tot,RCwater} \rho_{water} c_{p,water} + m_{Tot,steamwater} c_{p,water} = 3040 \left[\frac{MJ}{K} \right]$$

To ensure that the heat capacity factor isn't too low when using it for other plants than the 3 loops Westinghouse nuclear plant, the used heat capacity value is 3415.23 MJ/K.

Appendix C – Heat exchanger theory

The heat transfer across a surface is expressed as:

$$Q = UA\Delta T_m$$

where Q = heat transferred per unit time, [W]

U = the overall heat transfer coefficient, [W/m²°C]

A = heat- transfer area, [m²]

ΔT_m = the mean temperature difference, [°C]

The mean temperature difference is expressed as:

$$\Delta T_m = F_t \Delta T_{lm}$$

The log mean temperature difference is expressed as:

$$\Delta T_{lm} = \frac{(T_1 - t_2) - (T_2 - t_1)}{\ln \frac{(T_1 - t_2)}{(T_2 - t_1)}}$$

where T_1 = inlet shell-side fluid temperature

T_2 = outlet shell-side fluid temperature

t_1 = inlet tube-side temperature

t_2 = outlet tube-side temperature

F_t = the temperature correction factor

Note: The correction factor F_t is applied to flows which deviate from true counter-current flow.

For a two tube passes shell-and-heat exchanger the temperature correction factor is expressed as:

$$F_t = \frac{\sqrt{(R^2 + 1)} \ln \left[\frac{(1 - S)}{(1 - RS)} \right]}{(R - 1) \ln \left[\frac{2 - S \left[R + 1 - \sqrt{(R^2 + 1)} \right]}{2 - S \left[R + 1 + \sqrt{(R^2 + 1)} \right]} \right]}$$

where $R = \frac{(T_1 - T_2)}{(t_2 - t_1)}$

$$S = \frac{(t_2 - t_1)}{(T_1 - t_1)}$$

The correlation between heat transfer and total thermal resistance is termed overall heat transfer coefficient and is expressed as:

$$\frac{1}{U} = \frac{1}{h_o} + \frac{1}{h_{od}} + \frac{d_o \ln\left(\frac{d_o}{d_i}\right)}{2k_w} + \frac{d_o}{d_i} \times \frac{1}{h_{id}} + \frac{d_o}{d_i} \times \frac{1}{h_i}$$

where U = the overall heat transfer coefficient, [W/m²°C]

h_o = outside fluid film coefficient, [W/m²°C]

h_i = inside fluid film coefficient, [W/m²°C]

h_{od} = outside dirt coefficient – fouling factor, [W/m²°C]

h_{id} = inside dirt coefficient – fouling factor, [W/m²°C]

k_w = thermal conductivity of the tube wall material, [W/m°°C]

d_i = tube inside diameter, [m]

d_o = tube outside diameter, [m]

Kern's method – calculation of heat transfer coefficients for shell-and-tube heat exchangers.

The tube-side heat transfer coefficient is expressed as:

$$h_i = \frac{j_h k_f Re Pr^{0.33} \left(\frac{\mu}{\mu_w}\right)^{-0.14}}{d_i}$$

where μ_w = fluid viscosity at the wall, [Ns/m²]

μ = fluid viscosity at the bulk fluid temperature, [Ns/m²]

k_f = fluid thermal conductivity, [W/m°°C]

j_h = heat transfer factor (given in a graph)

The Prandtl number is expressed as:

$$Pr = \frac{c_p \mu}{k_f}$$

where c_p = fluid specific heat capacity, [J/kg°°C].

The Reynolds number is expressed as:

$$Re = \frac{\rho u_t d_e}{\mu}$$

where ρ = density [kg/m³]

$d_e = d_i$ for tubes [m]

u_t = fluid velocity [m/s]

For water, the heat transfer coefficient can be estimated more accurate by using a simplified equation:

$$h_i = \frac{4200(1.35 + 0.02t)u_t^{0.8}}{d_i^{0.2}}$$

where h_i = inside fluid film coefficient, [W/m²°C]

t = water temperature, [°C]

u_t = water velocity, [m/s]

d_i = tube inside diameter, [mm]

The procedure for calculating the shell-side heat transfer coefficient is more complex. The steps and expressions included are:

$$h_o = \frac{j_h k_f \text{Re Pr}^{\frac{1}{3}} \left(\frac{\mu}{\mu_w} \right)^{0.14}}{d_e}$$

where μ_w = fluid viscosity at the wall, [Ns/m²]

μ = fluid viscosity at the bulk fluid temperature, [Ns/m²]

k_f = fluid thermal conductivity, [W/m°C]

j_h = shell-side heat transfer factor (given in a graph)

The shell-side hydraulic diameter for an equilateral triangular pitch arrangement is expressed as:

$$d_e = \frac{4 \left(\frac{p_t}{2} \times 0.87 p_t - \frac{1}{2} \pi \frac{d_o^2}{4} \right)}{\pi \frac{d_o}{2}}$$

where p_t = tube pitch, [m]

d_o = tube outside diameter, [m]

The Reynolds number is expressed as:

$$\text{Re} = \frac{G_s d_e}{\mu}$$

The shell-side mass velocity is expressed as:

$$G_s = \frac{W_s}{A_s}$$

The area for cross flow is expressed as:

$$A_s = \frac{(p_t - d_o) D_s l_B}{p_t}$$

where D_s = shell inside diameter, [m]

l_B = baffle spacing, [m]

The Prandtl number is expressed as:

$$\text{Pr} = \frac{c_p \mu}{k_f}$$

where c_p = fluid specific heat capacity, [J/kg°C].

Appendix D – Auxiliary heat loads on CC-711

Apart from heat transferred via the RH-321 heat exchanger, the component cooling system supply cooling water to a number of other components presented in Table D.1-D.2. The heat load is defined for two operating points, 4 and 20 hours after reactor shutdown.

Table D.1 – Auxiliary heat load 4 hours after reactor shutdown.

Load description	Heat load [kW]
Letdown HX	3239
Excess Letdown HX	0
Seal Water HX	440
BTR Chiller Unit	480
Boron Recycle Evap.	0
Reactor Coolant Pumps	352
Sample HX	480
Spent Fuel Pit HX	805
Waste Gas Comp	79
Waste Evaporator	0
Containment Spray HX	0
Blowdown Cleanup Cooler	1595
R.C. Drain Tank HX	185
CC-711 pumps	620
Total load	8275

Table D.2 - Auxiliary heat loads 20 hours after reactor shutdown.

Load description	Heat load [kW]
Letdown HX	0
Excess Letdown HX	0
Seal Water HX	0
BTR Chiller Unit	0
Boron Recycle Evap.	0
Reactor Coolant Pumps	0
Sample HX	510
Spent Fuel Pit HX	805
Waste Gas Comp	40
Waste Evaporator	0
Containment Spray HX	0
Blowdown Cleanup Cooler	0
R.C. Drain Tank HX	0
CC-711 pumps	620
Total load	1975

Appendix E – MATLAB scripts

```
%% File name: RHCCSWsystem_initialization.m

% M-file containing constants for RHCCSWsystem.mdl
% Created by Jakob Dotevall & Jennie Nordkvist - Spring 2012

%% General input

%Salt water temperature
T_SW=25+273.15; % [K]

% Heat capacity of RC system - taken from "R3 GREAT Plant Input Data" page
76/99
% (Darwin ID 1906684)
C_RC=3.41523*1e9; % [J/K]

% DECAY HEAT CURVE
%Values taken from "Ringhals 3 GREAT - Decay heat models" (Darw.ID 1911580)
%Table 6.4.4-1, case A (12 month fuel cycle), corrected values (safety
factor of 1.111)
%The decay heat curve is interpreted by Simulink in every timestep, with
%linearization between known values.

h_ = 3600;
d_ = 24*h_;

% Decay heat [W] -
P_RC = [ 4*h_ , 30.39696e6; ...
        10*h_ , 24.00871e6; ...
        15*h_ , 21.54229e6; ...
        20*h_ , 19.89801e6; ...
        30*h_ , 17.69823e6; ...
        40*h_ , 16.20949e6; ...
        50*h_ , 15.08738e6; ...
        60*h_ , 14.19858e6; ...
        62*h_ , 14.03193e6; ...
        70*h_ , 13.45421e6; ...
        85*h_ , 12.53208e6; ...
        95*h_ , 12.00991e6; ...
        110*h_ , 11.34331e6; ...
        120*h_ , 10.95224e6; ...
        130*h_ , 10.59894e6; ...
        135*h_ , 10.4334e6; ...
        150*h_ , 9.980113e6; ...
        8*d_ , 8.969103e6; ...
        10*d_ , 8.128076e6; ...
        15*d_ , 6.809487e6; ...
        ];

% Auxiliary heat [W]
%Taken from "R3 GREAT Residual Heat Removal System..." (Darw.ID 1907420)???
%Interpreted by Simulink in every timestep, with linearization
%between known values.
P_CCEX = [4*h_ , 8.275e6; ...
          20*h_ , 1.975e6; ...
          30*h_ , 1.975e6];
```

```

% Heat generated by pumps
P_RCP = 4.4e6; % [W]
P_SWP = 200; % [W] Per pump. The full power is considered in the thermal
%balance (see FREJ). From Table 9.2.1-2, R3 SAR kap
9.2 (Darwin 1602715)

% Flow rates
q_RH = 234.36; % kg/s per train
q_CC = 504; % kg/s per train
q_CCRH = 252; % kg/s per train 252
q_SW_1 = 420; % kg/s per train (with one SW-pump per train in
operation)
q_SW_2 = 720; % kg/s per train (with two SW-pumps per train in
operation)

% Specific heat capacities
c_pCC = 4182.9; % Specific heat at 65 degrees Celcius/ 7 bars [J/kgK]
c_pSW = 4001.3; % Specific heat at 25 degrees Celcius [J/kgK]

% Initial temperatures
T_RC_start = 176.9+273.15; % [K]
T_RH_start = 127+273.15; % [K]
T_CC_start = 45+273.15; % [K]
T_CCR_start = 61+273.15; % [K]
T_CCRH_start = 92+273.15; % [K]
T_SWR_start = 40+273.15; % [K]

T_RH_B_start = T_RC_start; % [K]
T_CC_B_start = 40+273.15; % [K]
T_CCRH_B_start = 40+273.15; % [K]
T_SWR_B_start = 27+273.15; % [K]

% Initial guess for heat transfer capacity of CCAHCC-02
kA_CCAHCC_02 = 1728000; % [W/K]

%% Input to CCAHCC heat exchanger sub-model

length_tubeCC= 7162E-3; % [m]Tube length
t_thickCC=0.7E-3; % [m]Tube wall thickness
d_outCC=19.05E-3; % [m]Tube outer diameter
d_inCC=d_outCC-2*t_thickCC; % [m]Tube inner diameter
p_tCC=24E-3; % [m]Tube pitch 30 Degrees
d_sCC=1660E-3; % [m]Shell inner diameter
l_bCC=387E-3; % [m]Mean baffle spacing

k_wCC=16.4; % [W/mC]Thermal conductivity for tube
material Ti Gr.2

n_tubepluggedCC_A=0; %The number of plugged tubes in train A
n_tubepluggedCC_B=0; %The number of plugged tubes in train B

n_tubeCC=2442; %Number of tubes in the heat exchanger

p_SSCC=7; % [bar] Design pressure Shell-side
p_TSCC=3.1; % [bar] Design pressure Tube-side

%Design fouling values
RfSSCC=88*10^-6; % [m2*K/W]

```

```

RfTSCC=88*10^-6;           %[m2*K/W]

%% Input to RHAHRS heat exchanger sub-model

length_tubeRH=5.58;        %[m]Tube length
t_thickRH=1.22E-3;        %[m]Tube wall thickness
d_outRH=3/4*0.0254;       %[m]Tube outer diameter (3/4 inch, 1
inch=2.54 cm)
d_inRH=d_outRH-2*t_thickRH; %[m]Tube inner diameter
p_tRH=1.25*d_outRH;       %[m]Tube pitch

% Shell inner diameter and baffle spacing not used. A_s is instead
% calculated using the velocity in the design point.
d_sRH=1.0;                %[m]Shell inner diameter
l_bRH=0.44;               %[m]Baffle spacing

u_s_design=1.75;          %[m/s] - Velocity on shellside
                           %from "Heat exchanger performance"-
                           %document, found in 3C302.1 (i.e. archive)
rho_design=992.9896;      %[kg/m3] - Density component cooling water
q_CCRH_design=252;        %[kg/s] - Mass flow on shellside in the
design point

k_wRH=16;                 %[W/mC] tubmaterial is SA 249 TP304
according to darwin 1841818

n_tubepluggedRH_A=0;      %The number of plugged tubes in train A
n_tubepluggedRH_B=0;      %The number of plugged tubes in train B

n_passRH=2;               %Number of tube passes
n_tubeRH=415;             %Number of tubes

%Fouling values
RfSSRH=0.09/1000;         %[m2*K/W]
RfTSRH=0.05/1000;         %[m2*K/W]

%Correction factor used to find design UA-value.
h_SS_adj_RH = 0.82;

```


Appendix F – Simulink model layout

The layout of the Simulink model for Case 1 is presented in Figure F.1-F.5. The figures are named after their hierarchic position in the Model Browser, i.e. Main system / Subsystem1 / Subsystem 2. Note that the notations in model are somewhat different compared to the notations used in the report.

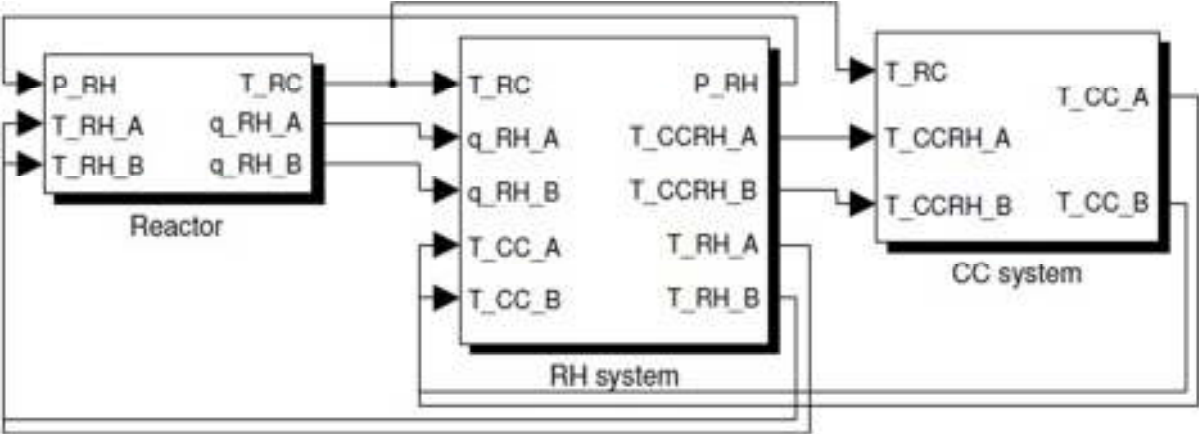


Figure F.1 – RHCCSWsystem.

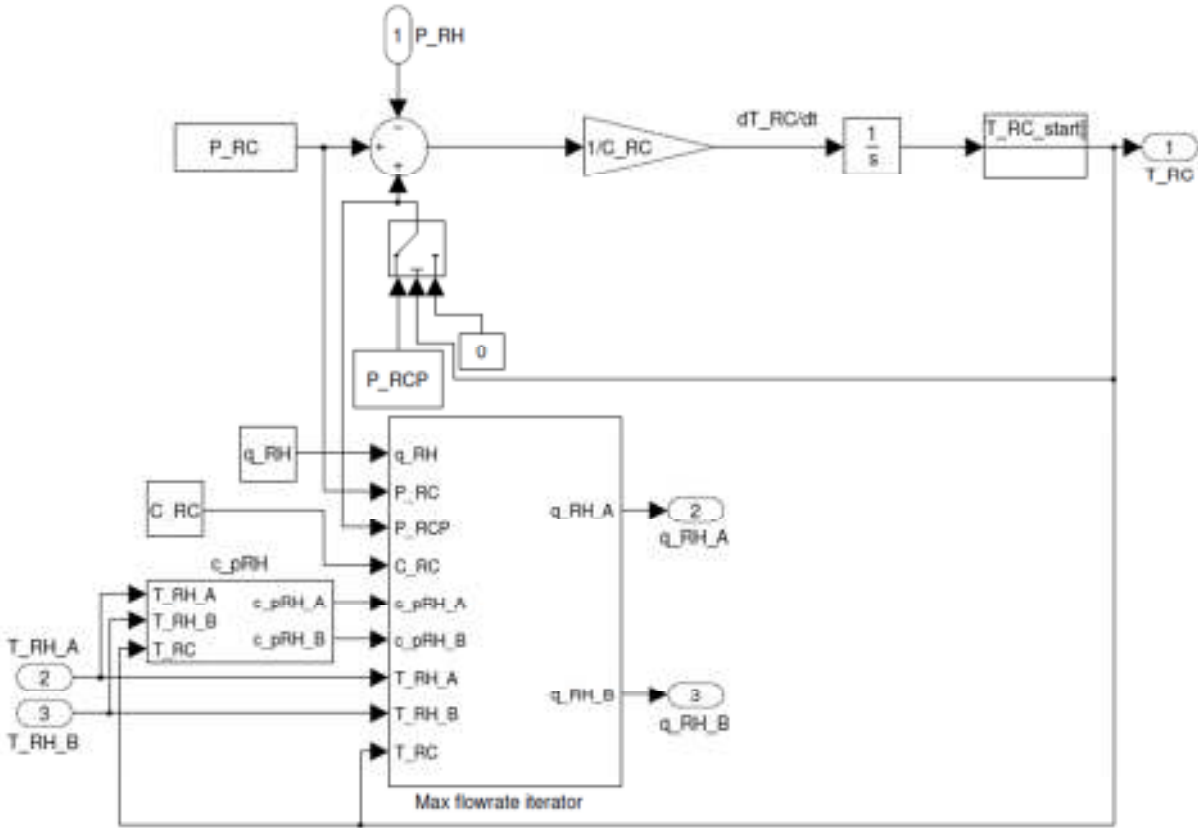


Figure F.2 - RHCCSWsystem / Reactor.

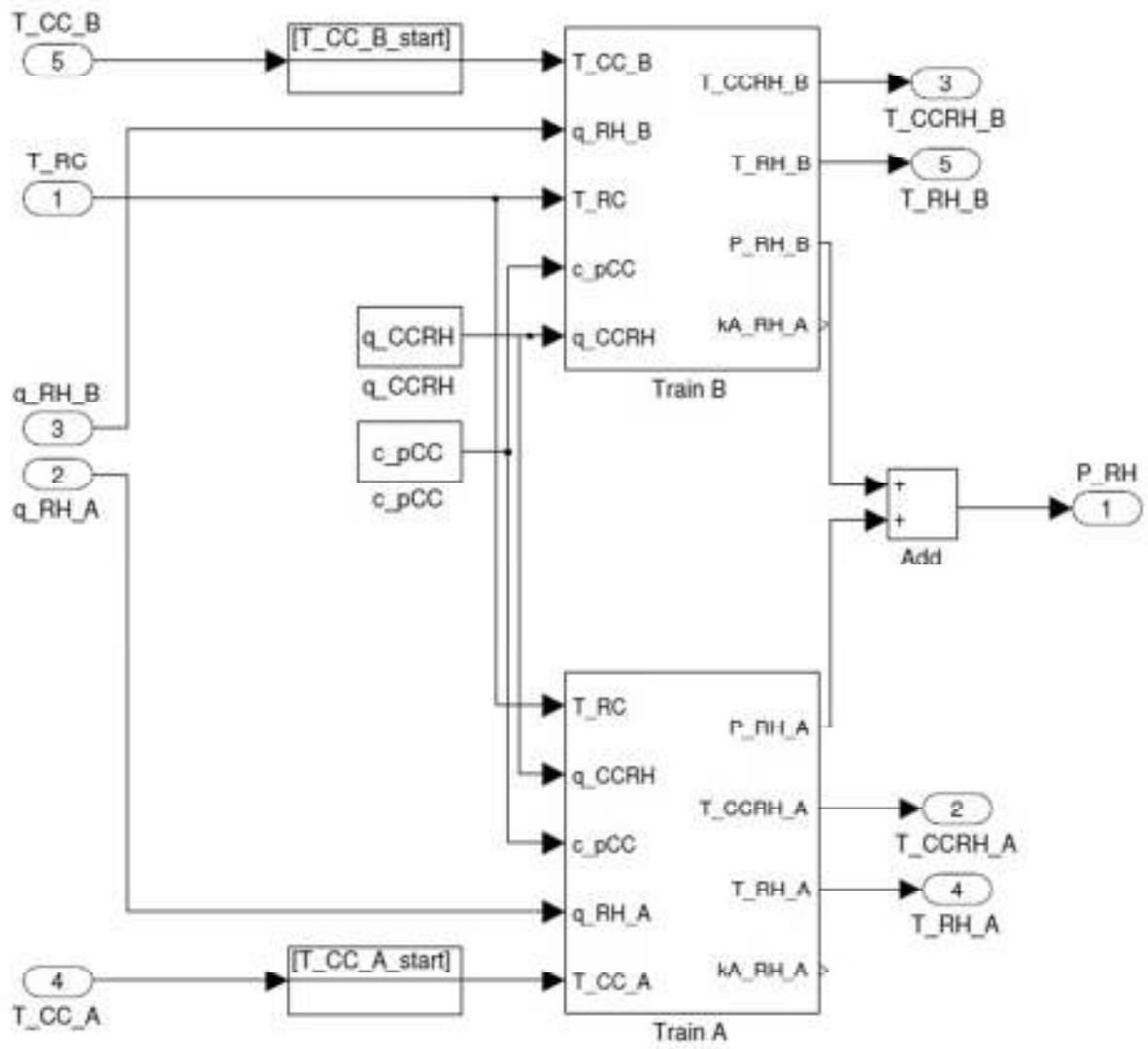


Figure F.3 - RHCCSWsystem / RH system.

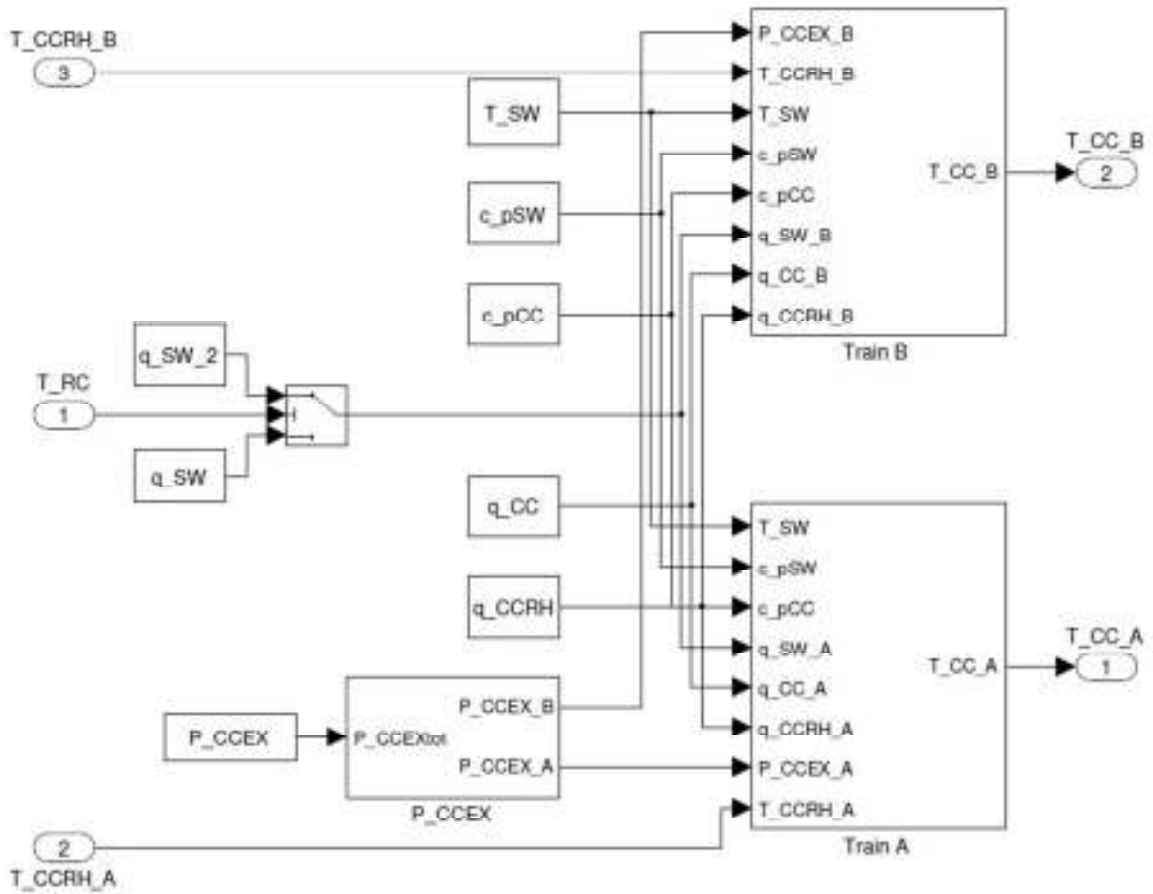


Figure F.4 - RHCCSWsystem / CC system.

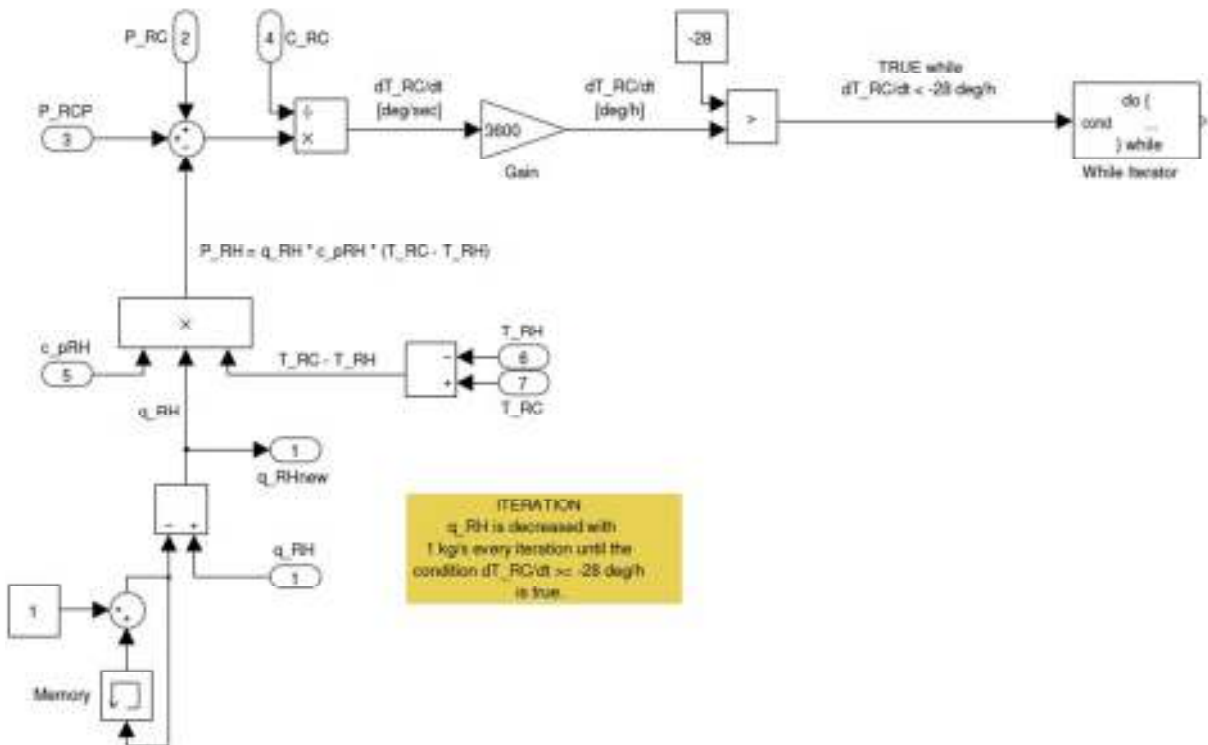


Figure F.5 - RHCCSWsystem / Reactor / ... / While Iterator.

Appendix G – Performance test

Table G.1 shows measured data from the performance test carried out 2007 and 2008. The measurements are denoted 1 to 12. This data has been used for validating the CC-711 heat exchanger sub-model. Table G.2 gives the tolerances that are used in the calculations.

Table G.1 – Measurements from the performance tests for the CC-711 heat exchangers.

Measurement	Shutdown	\dot{m}_{CC} [kg/s]	\dot{m}_{SW} [kg/s]	T_{CCR} [°C]	T_{CC} [°C]	T_{SW} [°C]	T_{SWR} [°C]	UA-value [kW/°C]
1	June 2007	246	424	26.4	21.3	19.5	21.8	1562 ±182
2	June 2007	505	723	23.5	21	19.3	20.9	2387 ±373
3	April 2008	212.5	480.3	26.5	14.0	10.2	15.53	1602 ±151
4	April 2008	435.2	469.8	20.8	14.7	10.3	15.3	2122 ±229
5	April 2008	596	470	19.5	15.1	10.3	15.4	2362 ±277
6	April 2008	433	377	21.6	15.7	10	16.3	1874 ±191
7	April 2008	434	692	19.1	13.1	10.1	13.7	2608 ±319
8	April 2008	250	519	25.9	16.2	12.5	16.9	1650 ±167
9	April 2008	440	518	22.8	16.9	12.6	17	2033 ±224
10	April 2008	585	518	23.1	18	12.7	17.7	2177 ±236
11	April 2008	439	329	25	19.3	12.6	19.2	1566 ±155
12	April 2008	441	744	21.6	15.7	12.7	15.6	2298 ±288

The UA-value is calculated in the following way:

$$Q_{CC} = \dot{m}_{CC} c_p (T_{CCR} - T_{CC})$$

$$Q_{SW} = \dot{m}_{SW} c_p (T_{SWR} - T_{SW})$$

$$Q_{mean} = \frac{Q_{CC}}{Q_{SW}}$$

$$UA = \frac{Q_{mean}}{\frac{(T_{CC} - T_{SW}) - (T_{CCR} - T_{SWR})}{\ln \frac{T_{CC} - T_{SW}}{T_{CCR} - T_{SWR}}}}$$

$c_p = 4.18 \text{ kJ/kg}^\circ\text{C}$ is used in calculations. The measurement uncertainties are calculated using a two-sided 95% confidence interval, and is based on the following tolerances:

Table G.2 – The tolerances used in the calculations.

	Tolerance
T_{CCR}	$\pm 0.2^{\circ}\text{C}$
T_{CC}	$\pm 0.2^{\circ}\text{C}$
T_{SW}	$\pm 0.2^{\circ}\text{C}$
T_{SWR}	$\pm 0.2^{\circ}\text{C}$
m_{CC}	$\pm 10\%$
m_{SW}	$\pm 10\%$

Appendix H – Simulation results

More simulation results are Figures H.1-H.3.

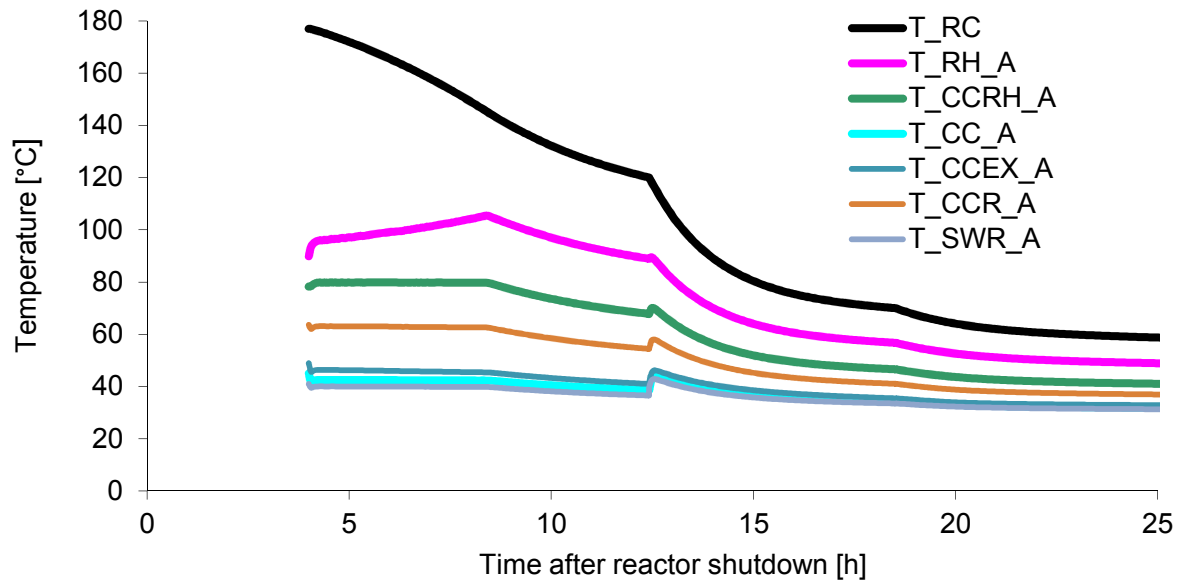


Figure H.1 - Simulated temperatures in train A, Case 1.

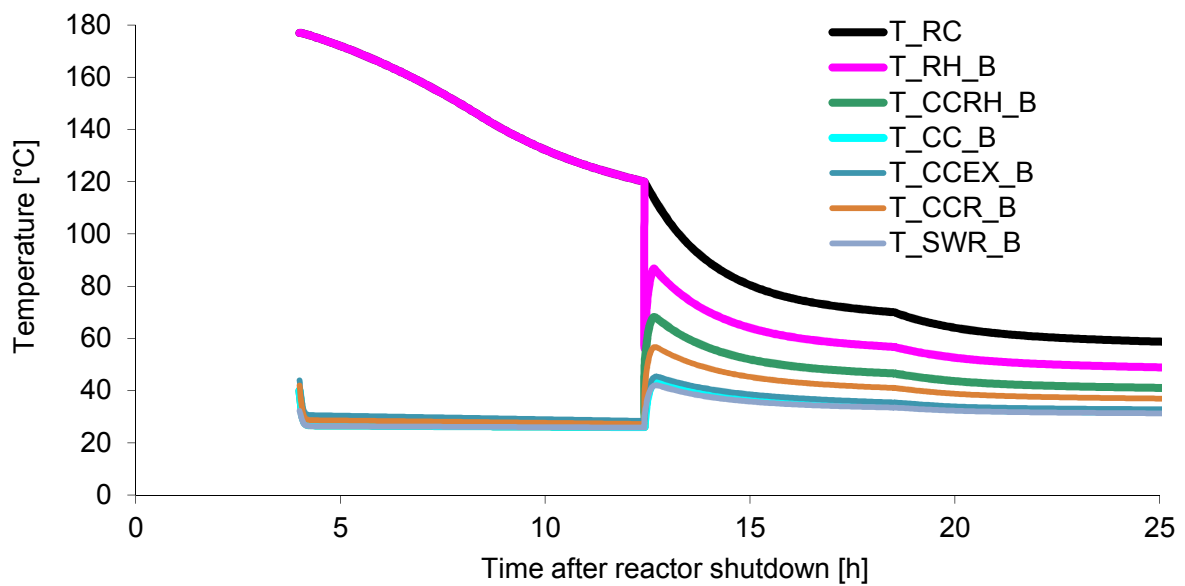


Figure H.2 - Simulated temperatures in train B, Case 1.

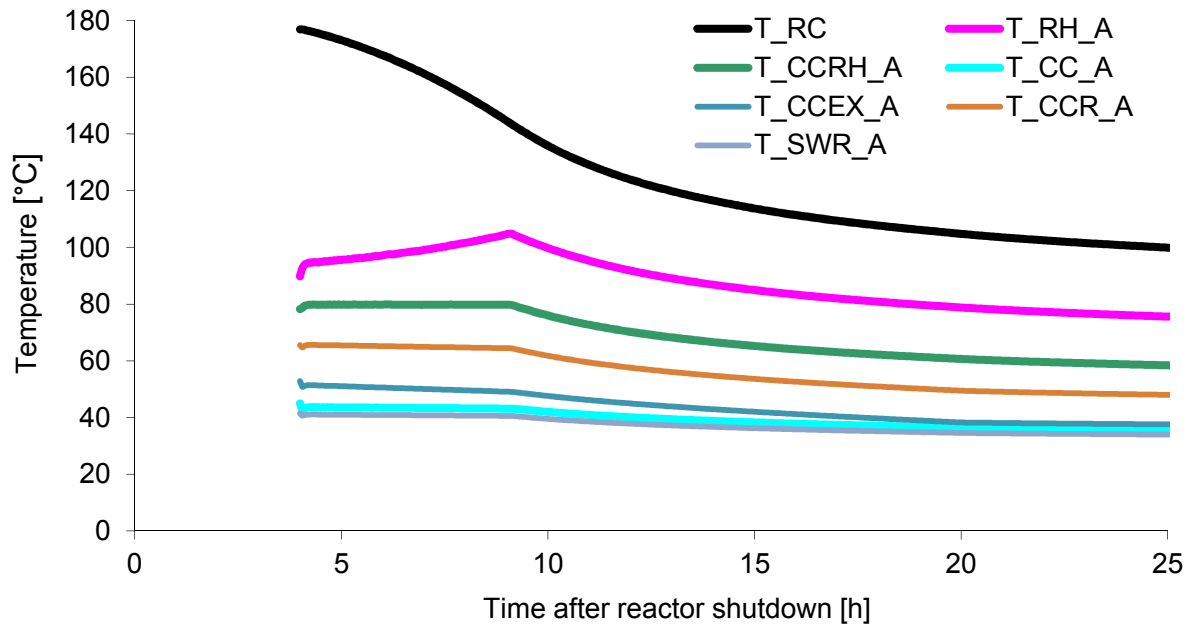


Figure H.3 - Simulated temperatures in train A, Case 2.